study of tributyltin chloride in female rats. J Toxicol Environ Health A 63:127–144
10. Boyer IJ 1989 Toxicity of dibutyltin, tributyltin and other organotin compounds to humans and to experimental animals. Toxicology 55:253–298
11. Heidrich DD, Steckelbroeck S, Klingmuller D 2001 Inhibition of human cytochrome P450 aromatase activity by butyltins. Steroids 66:763–769
12. Cooke GM 2002 Effect of organotins on human aromatase activity in vitro. Toxicol Lett 126:121–130
13. Powers MF, Beavis AD 1991 Triorganotins inhibit the mitochondrial inner membrane anion channel. J Biol Chem 266:17250–17256
14. Gennari A, Viviani B, Galli CL, Marinovich M, Pieters R, Corsini E 2000 Organotins induce apoptosis by disturbance of [Ca(2+)](i) and mitochondrial activity, causing oxidative stress and activation of caspases in rat thymocytes. Toxicol Appl Pharmacol 169:185–190
15. Philbert MA, Billingsley ML, Reuhl KR 2000 Mechanisms of injury in the central nervous system. Toxicol Pathol 28:43–53
16. Mu YM, Yanase T, Nishi Y, Waseda N, Oda T, Tanaka A, Takayanagi R, Nawata H 2000 Insulin sensitizer, troglitazone, directly inhibits aromatase activity in human ovarian granulosa cells. Biochem Biophys Res Commun 271:710–713
17. Mu YM, Yanase T, Nishi Y, Takayanagi R, Goto K, Nawata H 2001 Combined treatment with specific ligands for PPARγ:RXR nuclear receptor system markedly inhibits the expression of cytochrome P450arom in human granulosa cancer cells. Mol Cell Endocrinol 181:239–248
18. Saitoh M, Yanase T, Morinaga H, Tanabe M, Mu YM, Nishi Y, Nomura M, Okabe T, Goto K, Takayanagi R, Nawata H 2001 Tributyltin or triphenyltin inhibits aromatase activity in the human granulosa-like tumor cell line KGN. Biochem Biophys Res Commun 289:198–204
19. Nishikawa J, Mamiya S, Kanayama T, Nishikawa T, Shiraishi F, Horiguchi T 2004 Involvement of the retinoid X receptor in the development of imposex caused by organotins in gastropods. Environ Sci Technol 38: 6271–6276
20. Baillie-Hamilton PF 2002 Chemical toxins: a hypothesis to explain the global obesity epidemic. J Altern Complement Med 8:185–192
21. Heindel JJ 2003 Endocrine disruptors and the obesity epidemic. Toxicol Sci 76:247–249
22. Jacobs MN, Lewis DF 2002 Steroid hormone receptors and dietary ligands: a selected review. Proc Nutr Soc 61:105–122
23. Watanabe H, Iguchi T, Morohashi K 2002 [Endocrine disruptors and nuclear receptors]. Nippon Rinsho 60: 397–403
24. Kanayama T, Kobayashi N, Mamiya S, Nakanishi T, Nishikawa J 2005 Organotin compounds promote adipocyte differentiation as agonists of the peroxisome proliferator-activated receptor γ/retinoid X receptor pathway. Mol Pharmacol 67:766–774
25. Wang Z, Benoit G, Liu J, Prasad S, Aarnisalo P, Liu X, Xu H, Walker NP, Perlmann T 2003 Structure and function of Nurr1 identifies a class of ligand-independent nuclear receptors. Nature 423:555–560
26. Aarnisalo P, Kim CH, Lee JW, Perlmann T 2002 Defining requirements for heterodimerization between the retinoid X receptor and the orphan nuclear receptor Nurr1. J Biol Chem 277:35118–35123
27. Boehm MF, Zhang L, Zhi L, McClurg MR, Berger E, Wagoner M, Mais DE, Suto CM, Davies JA, Heyman RA, Nadzant AM 1995 Design and synthesis of potent retinoid X receptor selective ligands that induce apoptosis in leukemia cells. J Med Chem 38:3146–3155
28. Yu C, Chen L, Luo H, Chen J, Cheng F, Gui C, Zhang R, Shen J, Chen K, Jiang H, Shen X 2004 Binding analyses between human PPARγ-LBD and ligands. Eur J Biochem 271:386–397
29. Forman BM, Tontonoz P, Chen J, Brun RP, Spiegelman BM, Evans RM 1995 15-Deoxy-δ 12, 14-prostaglandin J2 is a ligand for the adipocyte determination factor PPAR γ. Cell 83:803–812
30. Schoonjans K, Staels B, Auwerx J 1996 The peroxisome proliferator activated receptors (PPARs) and their effects on lipid metabolism and adipocyte differentiation. Biochim Biophys Acta 1302:93–109
31. Kersten S 2002 Peroxisome proliferator activated receptors and obesity. Eur J Pharmacol 440:223–234
32. Lane MD, Tang QQ, Jiang MS 1999 Role of the CCAAT enhancer binding proteins (C/EBPs) in adipocyte differentiation. Biochem Biophys Res Commun 266:677–683
33. Tang QQ, Otto TC, Lane MD 2003 CCAAT/enhancer-binding protein β is required for mitotic clonal expansion during adipogenesis. Proc Natl Acad Sci USA 100: 850–855
34. Tang QQ, Lane MD 1999 Activation and centromeric localization of CCAAT/enhancer-binding proteins during the mitotic clonal expansion of adipocyte differentiation. Genes Dev 13:2231–2241
35. Rubin CS, Hirsch A, Fung C, Rosen OM 1978 Development of hormone receptors and hormonal responsiveness in vitro. Insulin receptors and insulin sensitivity in the preadipocyte and adipocyte forms of 3T3-L1 cells. J Biol Chem 253:7570–7578
36. Kletzien RF, Clarke SD, Ulrich RG 1992 Enhancement of adipocyte differentiation by an insulin-sensitizing agent. Mol Pharmacol 41:393–398
37. Kletzien RF, Foellmi LA, Harris PK, Wyse BM, Clarke SD 1992 Adipocyte fatty acid-binding protein: regulation of gene expression in vivo and in vitro by an insulin-sensitizing agent. Mol Pharmacol 42:558–562
38. Tafuri SR 1996 Troglitazone enhances differentiation, basal glucose uptake, and Glut1 protein levels in 3T3-L1 adipocytes. Endocrinology 137:4706–4712
39. Xue JC, Schwarz EJ, Chawla A, Lazar MA 1996 Distinct stages in adipogenesis revealed by retinoid inhibition of differentiation after induction of PPARγ. Mol Cell Biol 16:1567–1575
40. Kawada T, Kamei Y, Sugimoto E 1996 The possibility of active form of vitamins A and D as suppressors on adipocyte development via ligand-dependent transcriptional regulators. Int J Obes Relat Metab Disord 20(Suppl 3):S52–S57
41. Kawada T, Kamei Y, Fujita A, Hida Y, Takahashi N, Sugimoto E, Fushiki T 2000 Carotenoids and retinoids as suppressors on adipocyte differentiation via nuclear receptors. Biofactors 13:103–109
42. Tontonoz P, Graves RA, Budavari AI, Erdjument-Bromage H, Lui M, Hu E, Tempst P, Spiegelman BM 1994 Adipocyte-specific transcription factor ARF6 is a heterodimeric complex of two nuclear hormone receptors, PPAR γ and RXR α. Nucleic Acids Res 22:5628–5634
43. Martin G, Schoonjans K, Lefebvre AM, Staels B, Auwerx J 1997 Coordinate regulation of the expression of the fatty acid transport protein and acyl-CoA synthetase genes by PPARα and PPARγ activators. J Biol Chem 272:28210–28217
44. Motojima K, Passilly P, Peters JM, Gonzalez FJ, Latruffe N 1998 Expression of putative fatty acid transporter genes are regulated by peroxisome proliferator-activated receptor α and γ activators in a tissue- and inducer-specific manner. J Biol Chem 273:16710–16714
45. Frohnert BI, Hui TY, Bernlohr DA 1999 Identification of a functional peroxisome proliferator-responsive element in the murine fatty acid transport protein gene. J Biol Chem 274:3970–3977
46. Martin G, Poirier H, Hennuyer N, Crombie D, Fruchart JC, Heyman RA, Besnard P, Auwerx J 2000 Induction of the fatty acid transport protein 1 and acyl-CoA synthase

genes by dimer-selective rexinoids suggests that the peroxisome proliferator-activated receptor-retinoid X receptor heterodimer is their molecular target. J Biol Chem 275:12612–12618
47. Tontonoz P, Hu E, Devine J, Beale EG, Spiegelman BM 1995 PPAR γ 2 regulates adipose expression of the phosphoenolpyruvate carboxykinase gene. Mol Cell Biol 15:351–357
48. Magana MM, Lin SS, Dooley KA, Osborne TF 1997 Sterol regulation of acetyl coenzyme A carboxylase promoter requires two interdependent binding sites for sterol regulatory element binding proteins. J Lipid Res 38: 1630–1638
49. Schadinger SE, Bucher NL, Schreiber BM, Farmer SR 2005 PPARγ2 regulates lipogenesis and lipid accumulation in steatotic hepatocytes. Am J Physiol Endocrinol Metab 288:E1195–E1205
50. Tontonoz P, Kim JB, Graves RA, Spiegelman BM 1993 ADD1: a novel helix-loop-helix transcription factor associated with adipocyte determination and differentiation. Mol Cell Biol 13:4753–4759
51. Kim JB, Spiegelman BM 1996 ADD1/SREBP1 promotes adipocyte differentiation and gene expression linked to fatty acid metabolism. Genes Dev 10:1096–1107
52. Joseph SB, Laffitte BA, Patel PH, Watson MA, Matsukuma KE, Walczak R, Collins JL, Osborne TF, Tontonoz P 2002 Direct and indirect mechanisms for regulation of fatty acid synthase gene expression by liver X receptors. J Biol Chem 277:11019–11025
53. Seo JB, Moon HM, Kim WS, Lee YS, Jeong HW, Yoo EJ, Ham J, Kang H, Park MG, Steffensen KR, Stulnig TM, Gustafsson JA, Park SD, Kim JB 2004 Activated liver X receptors stimulate adipocyte differentiation through induction of peroxisome proliferator-activated receptor γ expression. Mol Cell Biol 24:3430–3444
54. Yu S, Matsusue K, Kashireddy P, Cao WQ, Yeldandi V, Yeldandi AV, Rao MS, Gonzalez FJ, Reddy JK 2003 Adipocyte-specific gene expression and adipogenic steatosis in the mouse liver due to peroxisome proliferator-activated receptor γ1 (PPARγ1) overexpression. J Biol Chem 278:498–505
55. Hallakou S, Doare L, Foufelle F, Kergoat M, Guerre-Millo M, Berthault MF, Dugail I, Morin J, Auwerx J, Ferre P 1997 Pioglitazone induces in vivo adipocyte differentiation in the obese Zucker fa/fa rat. Diabetes 46:1393–1399
56. de Souza CJ, Eckhardt M, Gagen K, Dong M, Chen W, Laurent D, Burkey BF 2001 Effects of pioglitazone on adipose tissue remodeling within the setting of obesity and insulin resistance. Diabetes 50:1863–1871
57. Smith SR, De Jonge L, Volaufova J, Li Y, Xie H, Bray GA 2005 Effect of pioglitazone on body composition and energy expenditure: a randomized controlled trial. Metabolism 54:24–32
58. Auwerx J 1999 PPARγ, the ultimate thrifty gene. Diabetologia 42:1033–1049
59. Ferre P 2004 The biology of peroxisome proliferator-activated receptors: relationship with lipid metabolism and insulin sensitivity. Diabetes 53(Suppl 1):S43–S50
60. Day C 1999 Thiazolidinediones: a new class of antidiabetic drugs. Diabet Med 16:179–192
61. Mukherjee R, Davies PJ, Crombie DL, Bischoff ED, Cesario RM, Jow L, Hamann LG, Boehm MF, Mondon CE, Nadzan AM, Paterniti Jr JR, Heyman RA 1997 Sensitization of diabetic and obese mice to insulin by retinoid X receptor agonists. Nature 386:407–410
62. Hill JO, Peters JC 1998 Environmental contributions to the obesity epidemic. Science 280:1371–1374
63. Barker DJ, Bull AR, Osmond C, Simmonds SJ 1990 Fetal and placental size and risk of hypertension in adult life. Br Med J 301:259–262
64. Phillips DI, Hirst S, Clark PM, Hales CN, Osmond C 1994 Fetal growth and insulin secretion in adult life. Diabetologia 37:592–596
65. Martyn CN, Barker DJ, Jespersen S, Greenwald S, Osmond C, Berry C 1995 Growth in utero, adult blood pressure, and arterial compliance. Br Heart J 73:116–121
66. Yajnik C 2000 Interactions of perturbations in intrauterine growth and growth during childhood on the risk of adult-onset disease. Proc Nutr Soc 59:257–265
67. Barker DJ, Martyn CN, Osmond C, Hales CN, Fall CH 1993 Growth in utero and serum cholesterol concentrations in adult life. Br Med J 307:1524–1527
68. Lucas A 1998 Programming by early nutrition: an experimental approach. J Nutr 128:401S–406S
69. Armitage JA, Khan IY, Taylor PD, Nathanielsz PW, Poston L 2004 Developmental programming of metabolic syndrome by maternal nutritional imbalance; how strong is the evidence from experimental models in mammals? J Physiol 561:355–377
70. Masuno H, Kidani T, Sekiya K, Sakayama K, Shiosaka T, Yamamoto H, Honda K 2002 Bisphenol A in combination with insulin can accelerate the conversion of 3T3-L1 fibroblasts to adipocytes. J Lipid Res 43:676–684
71. Masuno H, Okamoto S, Iwanami J, Honda K, Shiosaka T, Kidani T, Sakayama K, Yamamoto H 2003 Effect of 4-nonylphenol on cell proliferation and adipocyte formation in cultures of fully differentiated 3T3-L1 cells. Toxicol Sci 75:314–320
72. Toschke AM, Koletzko B, Slikker Jr W, Hermann M, von Kries R 2002 Childhood obesity is associated with maternal smoking in pregnancy. Eur J Pediatr 161:445–448
73. von Kries R, Toschke AM, Koletzko B, Slikker Jr W 2002 Maternal smoking during pregnancy and childhood obesity. Am J Epidemiol 156:954–961
74. Oken E, Huh SY, Taveras EM, Rich-Edwards JW, Gillman MW 2005 Associations of maternal prenatal smoking with child adiposity and blood pressure. Obes Res 13: 2021–2028
75. Power C, Jefferis BJ 2002 Fetal environment and subsequent obesity: a study of maternal smoking. Int J Epidemiol 31:413–419
76. Hill SY, Shen S, Locke Wellman J, Rickin E, Lowers L 2005 Offspring from families at high risk for alcohol dependence: increased body mass index in association with prenatal exposure to cigarettes but not alcohol. Psychiatry Res 135:203–216
77. Umesono K, Murakami KK, Thompson CC, Evans RM 1991 Direct repeats as selective response elements for the thyroid hormone, retinoic acid, and vitamin D3 receptors. Cell 65:1255–1266
78. Perlmann T, Rangarajan PN, Umesono K, Evans RM 1993 Determinants for selective RAR and TR recognition of direct repeat HREs. Genes Dev 7:1411–1422
79. Blumberg B, Mangelsdorf DJ, Dyck JA, Bittner DA, Evans RM, De Robertis EM 1992 Multiple retinoid-responsive receptors in a single cell: families of retinoid "X" receptors and retinoic acid receptors in the *Xenopus* egg. Proc Natl Acad Sci USA 89:2321–2325
80. Blumberg B, Bolado J Jr., Derguini F, Craig AG, Moreno TA, Chakravarti D, Heyman RA, Buck J, Evans RM 1996 Novel retinoic acid receptor ligands in *Xenopus* embryos. Proc Natl Acad Sci USA 93:4873–4878
81. Blumberg B, Sabbagh Jr W, Juguilon H, Bolado Jr J, van Meter CM, Ong ES, Evans RM 1998 SXR, a novel steroid and xenobiotic-sensing nuclear receptor. Genes Dev 12: 3195–3205
82. Tabb MM, Sun A, Zhou C, Grun F, Errandi J, Romero K, Pham H, Inoue S, Mallick S, Lin M, Forman BM, Blumberg B 2003 Vitamin K2 regulation of bone homeostasis is mediated by the steroid and xenobiotic receptor SXR. J Biol Chem 278:43919–43927
83. Grun F, Blumberg B 2003 Identification of novel nuclear hormone receptor ligands by activity-guided purification. Methods Enzymol 364:3–24
84. Grun F, Venkatesan RN, Tabb MM, Zhou C, Cao J, Hemmati D, Blumberg B 2002 Benzoate X receptors α

and β are pharmacologically distinct and do not function as xenobiotic receptors. J Biol Chem 277:43691–43697
85. Livak KJ, Schmittgen TD 2001 Analysis of relative gene expression data using real-time quantitative PCR and the 2(-Δ Δ C(T)) method. Methods 25:402–408
86. Bourguet W, Ruff M, Chambon P, Gronemeyer H, Moras D 1995 Crystal structure of the ligand-binding domain of the human nuclear receptor RXR-α. Nature 375:377–382
87. Allegretto EA, McClurg MR, Lazarchik SB, Clemm DL, Kerner SA, Elgort MG, Boehm MF, White SK, Pike JW, Heyman RA 1993 Transactivation properties of retinoic acid and retinoid X receptors in mammalian cells and yeast. Correlation with hormone binding and effects of metabolism. J Biol Chem 268:26625–26633
88. Lehmann JM, Moore LB, Smith-Oliver TA, Wilkison WO, Willson TM, Kliewer SA 1995 An antidiabetic thiazolidinedione is a high affinity ligand for peroxisome proliferator-activated receptor γ (PPAR γ). J Biol Chem 270: 12953–12956
89. Nieuwkoop P, Faber J 1994 Normal table of *Xenopus laevis* (Daudin). 2nd ed. New York: Garland Publishing, Inc.
90. Rugh R 1962 Experimental embryology: techniques and procedures. 3rd ed. Minneapolis: Burgess Publishing Co.

Molecular Endocrinology **is published monthly by The Endocrine Society (http://www.endo-society.org), the foremost professional society serving the endocrine community.**

Development 133, 1625-1634 (2006) doi:10.1242/dev.02344

Activation of Notch1 signaling in cardiogenic mesoderm induces abnormal heart morphogenesis in mouse

Yusuke Watanabe[1,*,†], Hiroki Kokubo[1,2,*], Sachiko Miyagawa-Tomita[3], Maho Endo[1], Katsuhide Igarashi[4], Ken ichi Aisaki[4], Jun Kanno[4] and Yumiko Saga[1,2,‡]

Notch signaling is implicated in many developmental processes. In our current study, we have employed a transgenic strategy to investigate the role of Notch signaling during cardiac development in the mouse. Cre recombinase-mediated Notch1 (NICD1) activation in the mesodermal cell lineage leads to abnormal heart morphogenesis, which is characterized by deformities of the ventricles and atrioventricular (AV) canal. The major defects observed include impaired ventricular myocardial differentiation, the ectopic appearance of cell masses in the AV cushion, the right-shifted interventricular septum (IVS) and impaired myocardium of the AV canal. However, the fates of the endocardium and myocardium were not disrupted in NICD1-activated hearts. One of the Notch target genes, *Hesr1*, was found to be strongly induced in both the ventricle and the AV canal of NICD1-activated hearts. However, a knockout of the *Hesr1* gene from NICD-activated hearts rescues only the abnormality of the AV myocardium. We searched for additional possible targets of NICD1 activation by GeneChip analysis and found that *Wnt2*, *Bmp6*, jagged 1 and *Tnni2* are strongly upregulated in NICD1-activated hearts, and that the activation of these genes was also observed in the absence of Hesr1. Our present study thus indicates that the Notch1 signaling pathway plays a suppressive role both in AV myocardial differentiation and the maturation of the ventricular myocardium.

KEY WORDS: Notch signaling, Heart formation, AV cushion, EMT

INTRODUCTION

The heart is the first functional organ to be formed during mouse development. Cardiac development is a complex process that requires myogenesis and morphogenesis to occur simultaneously with contractility. In addition, distinct cell populations have to be integrated in a temporally and spatially precise fashion. Cardiac mesoderm is specified in the anterior lateral mesoderm, which is a primary heart field, and then converges to form a linear heart tube along the ventral midline of the embryo. The heart tube grows rapidly in length through the addition of cells from the second heart field (Buckingham et al., 2005), and balloons to develop its atrial and ventricular compartments during looping. At the end of loop formation, the atria and ventricles are aligned and connected with each chamber through the atrioventricular (AV) canal. It has been suggested that the formation of this connection might involve rightward expansion of the AV canal (de la Cruz and Miller, 1968), leftward remodeling of the primary ventricular septum (Wenink, 1981) or reorganization of the AV myocardium (Kim et al., 2001a). The AV canal forms the AV cushions that are the primordia of the valves and membranous septae. They first become evident as localized swellings in the cardiac jelly, which are subsequently invaded by endothelial cells. The properties of both the AV endocardium and AV myocardium are distinctive in the AV canal. Recently, Notch signaling has been implicated in many aspects of heart development.

Notch is a transmembrane receptor and consists of several functional domains, a series of EGF and Notch/Lin12 repeats in the extracellular region, a transmembrane domain, a RAM domain, CDC10/ankyrin repeats and a PEST domain in the intracellular region (Reaume et al., 1992). Binding of Notch ligands, including delta-like (Dll) and jagged (Jag) proteins in mammals, to the corresponding Notch receptors leads to the stepwise cleavage of the receptor by specific proteases. As a result of this processing, the Notch intracellular domain (NICD) is released and transferred to the nucleus. The NICD then interacts with RBPjκ [also known as Su(H), CBF-1 and Lag-1; Rbpsuh – Mouse Genome Informatics], and regulates the transcription of the bHLH genes hairy/enhancer of split (*Hes*) and its related protein *Hesr* (also known as Hey, HRT, CHF, HERP), which then function as transcriptional suppressors of downstream targets (Artavanis-Tsakonas et al., 1999; Iso et al., 2003). In the mouse, *Notch1* begins to be expressed in the notochord and mesodermal tissues, including the posterior mesoderm, splanchnic mesoderm and extra-embryonic mesoderm at the primitive streak stage, and the *Notch1* expression profile in the heart is restricted to the endocardium by E8.0 (Williams et al., 1995). *Notch4* and one of its ligands, *Dll4*, are also expressed in the endocardium (Shirayoshi et al., 1997; Timmerman et al., 2004). *Notch2* expression in the heart cannot be detected by in situ hybridization during the early stages of development (Hamada et al., 1999), but the Notch2 protein is present in the atrial and ventricular myocardium at E13.5 (McCright et al., 2002). Although *Notch3* is expressed in the cardiogenic plate at the early headfold stage, it is no longer expressed at E8.0 (Williams et al., 1995).

Among the aforementioned Notch expression patterns, the restricted *Notch1* and *Notch4* expression in the endocardium during early heart development indicates that there is a crucial

[1]Division of Mammalian Development, National Institute of Genetics, Yata 1111, Mishima 411-8540, Japan. [2]Department of Genetics, The Graduate University for Advanced studies, Yata 1111, Mishima 411-8540, Japan. [3]Department of Pediatric Cardiology, The Heart Institute of Japan, Tokyo Women's Medical University, 8-1 Kawada-cho, Shinjyuku-ku Tokyo162-8666, Japan. [4]Cellular and Molecular Toxicology Division, National Institute of Health Sciences, 1-18-1 Kamiyohga, Setagaya-ku Tokyo 158-8501, Japan.

*These authors equally contributed to this work
†Present address: Department of Developmental Biology, Institute Pasteur, 25 rue du Dr Roux, 75015 Paris, France
‡Author for correspondence (e-mail: ysaga@lab.nig.ac.jp)

Accepted 23 February 2006

role for Notch signaling in endocardial development. Moreover, both *Notch1* and *Rbpsuh*-null mice have revealed in a previous study that Notch1/Rbpsuh signaling is essential for endocardial development and for EMT in the AV cushions (Timmerman et al., 2004). Recently, studies in human have shown that *Notch1* mutations cause defects in aortic valve formation (Garg et al., 2005). Moreover, the possible downstream target genes of Notch signaling, *Hesr1* and *Hesr2*, are crucial factors during cardiac development. These downstream genes show a complementary expression pattern in the heart: *Hesr1* is expressed in the atrium, outflow tract (OFT) and endocardium, and *Hesr2* is expressed in the ventricle (Leimeister et al., 1999; Nakagawa et al., 1999). *Hesr2*-null mice show defects in AV valve formation, and atrial and ventricular septal formation in the heart (Donovan et al., 2002; Gessler et al., 2002; Kokubo et al., 2004; Sakata et al., 2002). Intriguingly, *Hesr1/Hesr2* double knockout mice show a severe phenotype of impaired trabeculation, EMT and septation of the heart (Kokubo et al., 2005), although *Hesr1*-null mice do not show any detectable defects (Fischer et al., 2004; Kokubo et al., 2005).

The suppressive roles of Notch signaling have been reported during myocardial development in a number of different species. In *Xenopus* embryos, Notch signaling suppresses the expression of myocardial genes, as a result of which the heart precursor cells do not contribute to the myocardium (Rones et al., 2000). Similarly, in the *Drosophila* heart it has been shown that Notch activity, which is mediated by Su(H), prevents myocardial cell fate determination (Han and Bodmer, 2003; Park et al., 1998). Consistent with this finding, *Rbpsuh*-null ES cells show increased cardiomyogenic differentiation, which is likely to be due to the lack of Notch signaling (Schroeder et al., 2003). However, it is not yet clear whether Notch1 activity is involved in the determination of the cardiac fate in the mouse, as it is in both *Xenopus* and *Drosophila*.

A knockout strategy is both a straightforward and powerful method for elucidating gene function but transgenic strategies that use ectopic expression also yield valuable information. To elucidate the significance of the restricted Notch signaling in the endocardium, we investigated the effects of the forced expression of Notch1 in the myocardium, where the Notch signals are normally inactive. We speculated that this may provide an insight into the predominant expression of Notch1 in the endocardial cell lineage. For this purpose, we introduced NICD1 into the cardiac lineage of the mouse using the *Cre-loxP* system in *Mesp1-Cre* mice (in which a *Cre* recombinase gene is knocked into the *Mesp1* locus). Mesp1 is a bHLH transcription factor that is initially expressed in the invaginating mesoderm at the onset of gastrulation. Lineage analysis using *Mesp1-Cre* revealed that *Mesp1*-expressing cells mainly contribute to the endocardium and myocardium of the heart and to the endothelial cells of the embryonic and extra-embryonic blood vessels (Saga et al., 2000; Saga et al., 1999). The exception is observed in mesenchymal cells in the OFT derived from neural crest cells and some of the cells in the peripheral cardiac conduction system (Kitajima et al., 2006). In our present study, the expression of NICD1 in the entire cardiac lineage of the mouse has allowed us to determine the outcome of the forced expression of Notch1 in the myocardium lineage. The fates of the endocardium and myocardium were found not to be disrupted in NICD1-activated hearts but the forced activation of Notch signaling in myocardium results in the suppression of both the AV myocardial differentiation and the maturation of the ventricular myocardium.

MATERIALS AND METHODS

Generation of transgenic mice

The CAG-CAT-*NICD1* construct was generated by substituting *NICD1* (Takahashi et al., 2000) for β-galactosidase in the CAG-CAT-Z vector (Yamauchi et al., 1999). This construct was injected into fertilized eggs and permanent transgenic lines were established. The generation of *Mesp1-Cre* mice and *Hesr1*-null mice has been described previously (Kokubo et al., 2005; Saga et al., 1999). NICD1-activation of the cardiac lineage in mice was achieved by crossing CAG-CAT-*NICD1* mice with *Mesp1-Cre* mice. A TOPGal transgenic mouse line was established by injection of a vector containing *E. coli* β-galactosidase with the TOPflash promoter-enhancer (Upstate).

Histological analyses

For histological observations, Hematoxylin and Eosin staining was conducted on paraffin sections and ultrastructures were then observed by transmission electron microscopy (Miyagawa-Tomita et al., 1996). In situ hybridization analyses were performed using cRNA probes for *Notch1*, *Jag1*, *Bmp6*, *Hesr1*, *Hesr2*, troponin 1 fast-twitch skeletal muscle isoform (*Tnni2*), *Wnt2*, *Anf*, chisel (*Smpx* – Mouse Genome Informatics), *Bmp2*, *Tbx2*, *Cited1*, *Hand1* and *Bmp10*. The InsituPro system (M&S Instruments) was used for whole-mount in situ hybridizations according to the manufacture's instructions. Section in situ hybridizations were performed using 20 μm frozen sections. Activated-Notch1 was detected using an anti-cleaved Notch1 antibody (Val1744) (#2421, Cell Signaling Technology) with 6 μm paraffin sections. Other immunohistochemical detections were performed using anti-Myosin (Skeletal, Slow) (#M8421, Sigma) which is highly specific for the slow myosin heavy chain (Mhc), anti-α Smooth Muscle Actin (αSma) (#A2547, Sigma) and anti-CD31 (Pecam-1) (#557355, BD Biosciences) antibodies with 8 μm frozen sections.

RT-PCR analysis

Total RNA was isolated from the atria and ventricles of E10.5 mouse hearts using an RNeasy mini kit (Qiagen). cDNA was generated using SuperScript II reverse transcriptase (Invitrogen). PCR was performed using primers for *Hesr1* (5′-ACGACATCGTCCCAGGTTTTG-3′ and 5′-GGTGATCCAC-AGTCATCTGCAAG-3′), *Hesr2* (5′-GCTACAAGCTCAGTGATGAGG-3′ and 5′-GCCTGGAGCATCTTCAAATGATCC-3′), *Hes1*, *Hes5* (Kaneta et al., 2000), *Tnni2* (5′-CCAGCACTGCTGCACAGCA-3′ and 5′-AGACATGGAGCCTGGGATG-3′), *Wnt2* (Monkley et al., 1996), *Bmp6* (5′-AGCAACTAGCAATCTGTGGG-3′ and 5′-CGTTGTAGTCTGAA-GAACCG-3′) and *Jag1* (Timmerman et al., 2004). The number of PCR cycles was optimized for each reaction.

GeneChip analysis

Ventricles with an AV canal were isolated at developmental stage E10.5 and stabilized in RNA*later* RNA Stabilization Reagent (Ambion), prior to total RNA preparation. Total RNA isolates were purified using the RNeasy mini kit (Qiagen), according to the manufacturer's instructions. First-strand cDNAs were synthesized by incubating 5 μg of total RNA with 200 U SuperScript II reverse transcriptase (Invitrogen) and 100 pmol T7-$(dT)_{24}$ primer [5′-GGCCAGTGAATTGTAATACGACTCACTATAGGGAGG-CGG-$(dT)_{24}$-3′]. After second-strand synthesis, the double-stranded cDNAs were purified using a GeneChip Sample Cleanup Module (Affymetrix), according to the manufacturer's instructions. Labeling of the double-stranded cDNAs was achieved by in vitro transcription using a BioArray HighYield RNA transcript labeling kit (Enzo Diagnostics, Farmingdale, NY). The labeled cRNA was then purified using a GeneChip Sample Cleanup Module (Affymetrix) and treated with 1× fragmentation buffer (40 mM acetate, 100 mM KOAc, 30 mM MgOAc) at 94°C for 35 minutes. For hybridization to a GeneChip Mouse Genome 430 2.0 Array (Affymetrix), 15 μg of fragmented cRNA probe was incubated with 50 pM control oligonucleotide B2, 1× eukaryotic hybridization control (1.5 pM BioB, 5 pM BioC, 25 pM BioD and 100 pM Cre), 0.1 mg/ml herring sperm DNA, 0.5 mg/ml acetylated BSA and 1× manufacturer-recommended hybridization buffer in a 45°C rotisserie oven for 16 hours. Washing and staining were performed with GeneChip Fluidic Station (Affymetrix) using the appropriate antibody amplification, washing and staining protocol. The phycoerythrin-stained arrays were scanned as digital image files and scanned

data were analyzed with GeneChip Operating Software (Affymetrix). The GeneChip analyses were performed using two different RNA samples prepared from the control and NICD1-activated hearts, respectively. All data are available online (http://www.nihs.go.jp/tox/TtgSubmitted.htm) in the National Institute of Health Sciences.

RESULTS

Notch1 signal activation in the cardiac cell lineage of the mouse induces heart abnormalities

To investigate the possible role of Notch1 signaling during cardiac development in the mouse, we generated a transgenic line expressing *NICD1* cDNA, which comes under the control of the CAG promoter after excision of the floxed CAT gene by Cre recombinase (designated as CAG-CAT-*NICD1* mice). We used *Mesp1-Cre* mice to induce NICD expression in the cardiac cell lineage in transgenic progeny. By crossing with *Mesp1-Cre* mice, Cre/lox specific CAT excision occurs in *Mesp1*-expressing cells and results in the induction of *NICD1*-expression in the cardiac lineages (designated as NICD1-activated mice). Whole-mount in situ hybridization experiments subsequently revealed a appreciable level of *Notch1* induction in the hearts of NICD1-activated mice (NICD1-activated hearts), which exhibited a deformed shape with a rough surface morphology (Fig. 1C,D). The transgenic mice did not develop beyond embryonic day 10.5 (E10.5) and died before E11.5. These heart abnormalities are clearly distinguishable from wild-type mice (Fig. 1A,B).

To confirm Notch1 activation, we performed immunohistochemical staining using antibodies against processed-NICD1. In wild-type hearts, Notch1 activation was observed only in the endocardium (Fig. 1E-H), but neither in myocardium or mesenchymal cells derived from the endocardium of the AV canal. By contrast, activated Notch1 was observed in the entire heart, including the endocardium, the myocardium of both the atria and ventricles, and the AV cushions, in NICD1-activated embryos (Fig. 1I-L). We were therefore able to conclude that Notch activation was successfully induced in the entire cardiac lineage in our double transgenic mice.

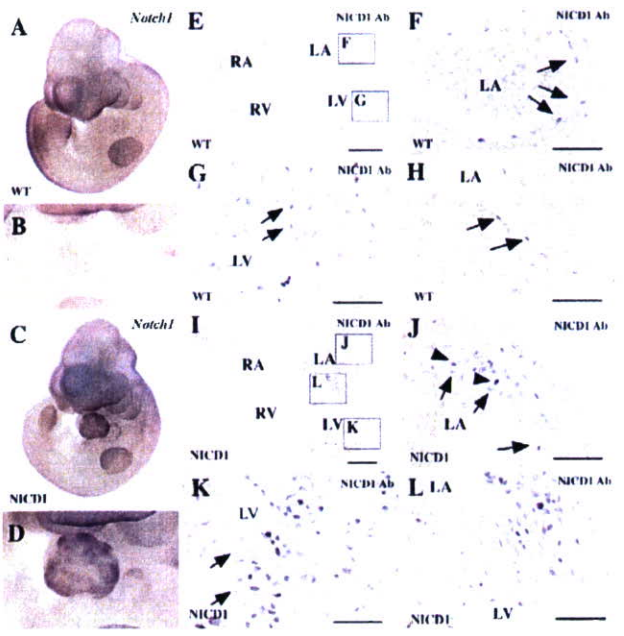

Fig. 1. Notch activation in the mouse cardiac cell lineage. (**A-D**) *Notch1* expression revealed by whole-mount in situ hybridization at E10.5. In wild-type embryos (A,B), it is difficult to detect Notch1 expression in the heart at the whole-mount level, whereas in NICD1-activated hearts (C,D), *Notch1* is strongly induced in whole heart which shows an abnormal morphology. The heart regions are magnified (B,D). (**E-L**) Immunohistochemical analysis of cleaved-Notch1 (NICD1 Ab) at E10.5. NICD1 signals are only observed in the nuclei of endocardial cells in the wild-type heart (E-H), whereas the signals are observed in both endocardial and myocardial cells in NICD1-activated hearts (I-L). The images of other sections were generated to indicate that only endocardial cells are NICD1-positive in the AV cushion of the wild-type embryonic heart (H). Arrows indicate endocardial cells. Arrowheads indicate myocardial cells. Abbreviations: LA, left atrium; RA, right atrium; LV, left ventricle; RV, right ventricle. Scale bars: 200 μm in E,I; 50 μm in F-H,J-L.

Myocardial defects in the NICD1-activated heart

Histological observations by H&E staining, followed by marker analyses, revealed four major defects in NICD1-activated hearts: (1) impaired ventricular myocardial differentiation; (2) the ectopic appearance of cell masses in the AV cushion; (3) right-shifted IVS; and (4) impaired myocardium of the AV canal. Aberrant myocardial trabeculation was the first anomaly to be observed (Fig. 2A,B). In the wild-type mouse heart, the trabeculae extend to the inner space of the ventricle from the compact layer that has a thickness of two to three cells (Fig. 2A). By contrast, the trabeculae were found to have accumulated in the ventricular wall in NICD1-activated hearts (Fig. 2B). The abnormal accumulation of trabecular cells near the compact layer is likely to be the cause of the rough external appearance of the ventricle (Fig. 1D). To investigate possible alterations in the properties of the trabecular cells in the NICD1-activated heart, we examined the expression of *Bmp10*, which is a gene that is known to be specifically expressed in the trabecular cells and to be important for the growth of trabecular myocardium (Fig. 2C) (Neuhaus et al., 1999). *Bmp10* expression was detected in the NICD1-activated heart, indicating that the trabecular cells were not strongly affected by Notch1 activation (Fig. 2D). However, this expression was not detected in the trabeculae of the AV myocardium (asterisk in Fig. 2D) (see below).

To examine the possibility that Notch1 signaling influences the fate decisions of the myocardium in mouse, as is the case in *Drosophila* and *Xenopus* (Han and Bodmer, 2003; Rones et al., 2000), we analyzed the expression of cell-type specific markers by RT-PCR and immunohistochemical staining. Semi-quantitative RT-PCR analysis showed no detectable changes in the expression of the myocardial genes, myosin light chain (*Mlc*) 2a (*Myl7* – Mouse Genome Informatics), *Mlc2v* (*Myl2* – Mouse Genome Informatics), *Mhca* (*Myh6* – Mouse Genome Informatics), *Nkx2.5*, *Mef2c* and *Gata4* in the ventricle (see Fig. S1 in the supplementary material). Although *Mhcb* (*Myh7* – Mouse Genome Informatics) appears to be induced in the atrium of NICD1-activated hearts, this might be due to contamination of the expanded left ventricle. We also examined protein markers such as Mhc, αSma (for myocardium) and Pecam (for endocardium) using specific antibodies. Although we found no significant changes in the expression patterns of Mhc and αSma, except for the AV canal (Fig. 2F, H, see below), Pecam expression was significantly reduced in the endocardium surrounding the trabecular cells in NICD1-activated hearts (Fig. 2J). Furthermore, Pecam-positive cells were often observed in the interventricular septum (IVS, see arrowheads in Fig. S2 in the supplementary material),which may indicate anomalies in the myocardium of the IVS. To further investigate these transgenic embryos for possible defects in the trabecular cells, we examined their fine structures by

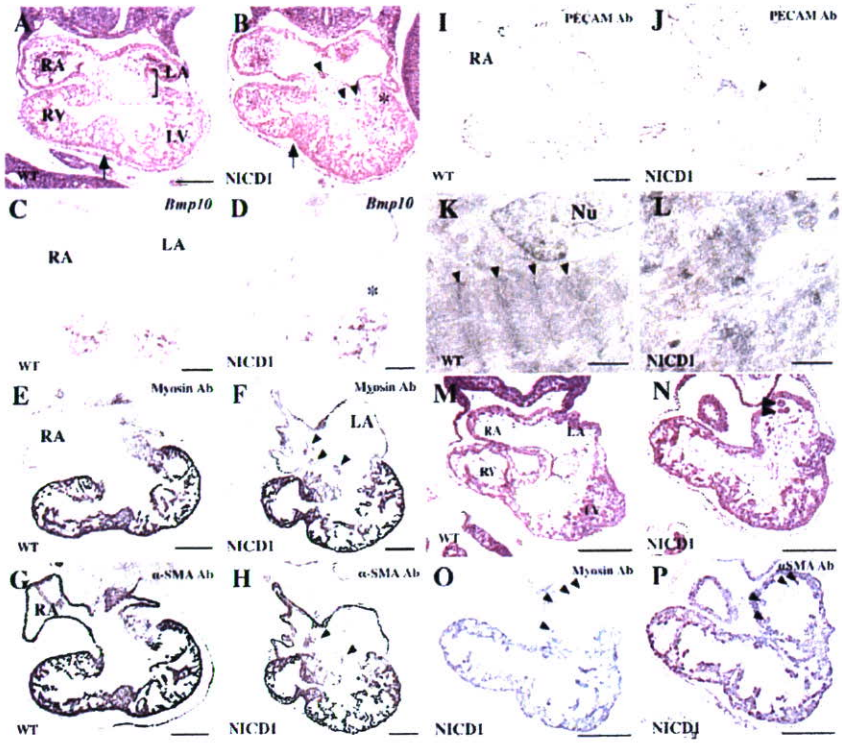

Fig. 2. Morphological and histological defects induced by NICD1-activation. (**A**,**B**) Sections stained with Hematoxylin and Eosin show normal EMT in the AV cushion (brackets) and trabecular development in wild-type hearts (A), whereas the trabeculae are not formed normally in NICD1-activated hearts (B). Ectopic cell masses were also evident (arrowheads in B), the interventricular septum is right-shifted (arrow) and trabeculation occurs in the AV myocardium (asterisk in B) in NICD1-activated hearts. (**C**,**D**) *Bmp10* expression was observed in the trabecular cells in both the wild-type (C) and NICD1-activated (D) ventricles. (**E-J**,**O**,**P**) Immunohistochemistry using anti-myosin (E,F,O), anti-α-smooth muscle actin (αSma) (G,H,P) and anti-Pecam (I,J) antibodies reveal that ectopic cell masses (arrowheads) are present in the cushion tissue in NICD1-activated hearts (F,H,J,O,P), but are never observed in wild-type hearts (E,G,I). (**M**,**N**) Hematoxylin and Eosin staining at E9.5 also shows ectopic cell masses in the cushion of NICD1-activated heart (arrowheads in N) but not in wild-type heart (M). (**K**,**L**) In wild-type myocardium (K), myofibrils with sarcomere structures (Z bands are indicated by black arrowheads) are observed by transmission electron microscopy, but only thin myofibrils without a proper sarcomere structure (no Z band indicated by while arrowheads) are formed in NICD1-activated hearts (L). Embryo samples were prepared at either E10.5 (A-L) or E9.5 (M-P). Serial sections were used for E,G,I (wild-type), F,H,J (NICD1-activated) and N-P (NICD1-activated). Abbreviations: LA, left atrium; RA, right atrium; LV, left ventricle; RA, right ventricle; Nu, nucleus. Scale bars: 200 μm in A-J,M-P; 1 μm in K,L.

transmission electron microscopy. At this stage, myofibrils are found to be well developed in the wild-type mouse heart and the sarcomere structures with Z bands were well organized in the wild-type trabecular myocardial cells (Fig. 2K). In NICD1-activated hearts, however, the myofibrils were poorly formed with an unclear sarcomere structure (Fig. 2L), indicating that myocardial maturation is inhibited in NICD1-activated hearts. These results indicate that Notch1 signaling does not influence the fate of myocardial cells in the mouse, but it acts as an inhibitor of myocardial differentiation, which is associated with abnormal trabeculation in the ventricle.

Appearance of ectopic cell masses in the AV cushion in the NICD1-activated heart

The second principal anomaly of the NICD1-activated heart that we observed occurs in the AV cushion. For the formation of the AV cushion, a subset of endocardial cells that overlie the AV canal undergoes endothelial-mesenchymal transformation (EMT), followed by invasion of the cardiac jelly. In NICD1-activated hearts, mesenchymal cells in the AV cushion were found, indicating that EMT events seemed to occur normally. However, ectopic cell masses were detected in the cushion tissue (Fig. 2B, arrowheads). Immunohistochemical analyses identified that these cell masses were Mhc- and αSma-positive (arrowheads in Fig. 2F,H), but Pecam negative (arrowhead in Fig. 2J), suggesting that these cells possess myocardial properties. It is noteworthy that these cells were never observed in wild-type cushion tissues at E10.5 (Fig. 2E,G). To determine how such ectopic cells develop in the NICD1-activated heart, we observed then at E9.5, when it is known that EMT starts to occur in the AV cushion. As is clearly shown in Fig. 2N, we found ectopic cell masses, which were Mhc- and αSma-positive (Fig. 2O,P), in the NICD1-activated heart but not in the wild-type samples (Fig. 2M). Furthermore, serial Hematoxylin and Eosin staining of sections along the AP axis indicated that these cells were derived from the myocardial cells located at the AV canal, where trabeculation does not generally occur at this stage (see Fig. S3 in the supplementary material).

IVS shift and AV myocardial defect in the NICD1-activated heart

The third anomaly of the NICD1-activated mouse heart is the noticeable difference in the size of the ventricles. The left ventricle in the NICD1-activated mouse appears to be expanded, whereas the

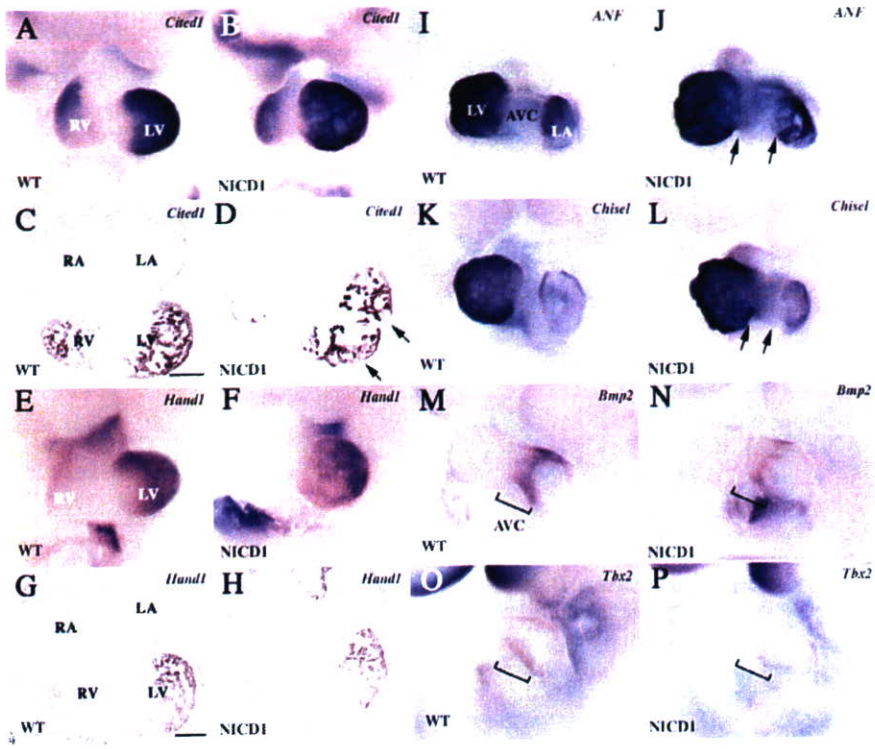

Fig. 3. Molecular characterization of defects in NICD1-activated hearts. The differences between the right and left ventricles were examined by whole mount (A,B,E,F) or section (C,D,G,H) in situ hybridization using probes *Cited1* (**A-D**) or *Hand1* (**E-H**). To demarcate the boundaries between both the atrial and ventricular chambers and the AV canal, chamber markers *Anf* (**I,J**), *Smpx* (**K,L**) and AV canal markers *Bmp2* (**M,N**) and *Tbx2* (**O,P**) were used as probes. Boundaries between the chambers and AV canal became less evident in the NICD1-activated heart (indicated by arrows in J and L). AV canal marker expression is also downregulated in the NICD1-activated hearts (indicated by brackets in M-P). Abbreviations: LA, left atrium; RA, right atrium; LV, left ventricle; RA, right ventricle. Scale bars: 200 μm in C,G.

right ventricle is reduced in size, compared with wild type. In addition, the position of the IVS that separates the right and left ventricles is shifted to the right side in the NICD1-activated mouse (compare arrows in Fig. 2A with 2B). However, no enhanced cell proliferation was observed in the left ventricles of NICD-activated hearts (data not shown), indicating that the property of each ventricle might be affected by Notch1 activation. The expression of *Cited1*, which is negative in the IVS, revealed differences in size between the right and left ventricles (Fig. 3A-D). We found cells showing reduced *Cited1* expression in the NICD1-activated heart (arrows in Fig. 3D), which may indicate abnormalities in cardiomyocyte differentiation. Furthermore, the expression of *Hand1*, which is a known marker for the left ventricle (Fig. 3E,G), showed expanded expression in the NICD1-activated heart (Fig. 3F,H).

It was also noted that the AV myocardial wall shows evidence of trabeculation in NICD1-activated mice (Fig. 2B,D,F,H,J,N,O,P; Fig. 3D,H). The properties of the chamber and AVC region were examined by molecular analyses using the chamber markers *Anf* and *Smpx* (*Chisel*) to demarcate the ventricles and atria (Fig. 3I-L), and *Bmp2* and *Tbx2* to characterize the AV canal (Fig. 3M-P). In the NICD1-activated heart, AVC marker expression, *Tbx2* in particular, is greatly reduced (Fig. 3P). In addition, the *Anf* and *Smpx* expression patterns revealed enlarged left ventricles and ambiguous AV boundaries (arrows in Fig. 3J,L). In the wild-type heart, the AV canal allows the endocardium to develop AV cushion tissue by EMT (Fig. 2A, brackets) and even though the AV myocardium shows weak Mhc and αSma staining in the wild-type heart (Fig. 2E,G), the trabeculae never develop in the AV myocardium at this stage. This indicates that the properties of the AV myocardium are distinct from the chamber myocardium. However, in the NICD1-activated heart, AV cushion tissues were formed and the trabeculae could be observed in the expected AV canal, which may indicate a lack of AV myocardial characteristics (Fig. 2B, asterisk).

Hesr1 is ectopically induced in the NICD1-activated ventricle

Hes and Hesr family members are known to be downstream targets of Notch signaling (Iso et al., 2003). We therefore examined whether these genes are induced in NICD1-activated hearts. RT-PCR and in situ hybridization analyses revealed that the expression of *Hesr1* and *Hesr2* is restricted to the myocardium of the atria and ventricles of wild-type hearts, respectively (Fig. 4A,B,D), which is consistent with previous reports (Leimeister et al., 1999; Nakagawa et al., 1999). However, in NICD1-activated hearts, *Hesr1* was found to be ectopically induced at high levels in the myocardium of the ventricle (Fig. 4A,C), whereas *Hesr2* was not shown to be induced in the myocardium of the atrium (Fig. 4A,E). Intriguingly, *Hesr1* was not expressed in the endocardium at this stage, despite the activation of Notch1 (Fig. 4B, Fig. 1G). A noticeable change was also observed in the AV myocardium of the transgenic hearts, in which the extended trabeculation appeared to be coincident with the co-expression of *Hesr1* and *Hesr2*. As *Hesr2* expression occurs in the wild-type ventricle, ectopic *Hesr1* expression might be the cause of the ventricle and AV canal defects in the NICD1-activated mice. In addition, *Hes5* expression was induced in both the atria and ventricles in Notch1-activated hearts (Fig. 4A), although it is not expressed in the wild-type heart.

NICD1 activation in a *Hesr1*-null background rescues the AV myocardium defect

Hesr1 is strongly induced in the NICD1-activated mouse heart and is known to be a transcriptional repressor, which lead us to hypothesize that the major cardiac defects observed in NICD1-activated mice might be caused by the ectopic expression of *Hesr1*. To examine this possibility, we generated NICD1-activated mice in a *Hesr1*-null background. *Hesr1* knockout mice show no detectable defects in heart morphogenesis (Fig. 5A,C,E) (Kokubo et al., 2005).

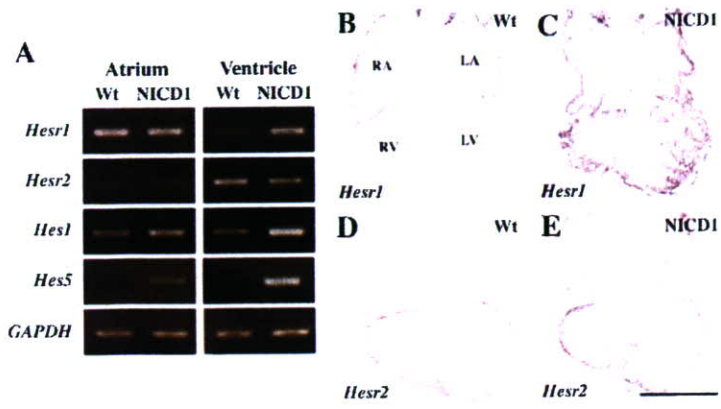

Fig. 4. Expression changes in the *Hes* and *Hesr* gene families at E10.5. (**A**) Semi-quantitative RT-PCR analysis showing upregulation of *Hesr1*, *Hes1* and *Hes5* in NICD1-activated hearts. *Hesr1* is ectopically induced at particularly high levels in the ventricle. In situ hybridization analysis also revealed the ectopic induction of *Hesr1* in the ventricle and AV canal of NICD1-activated hearts (**C**), whereas *Hesr1* is expressed only in the atrium in wild-type hearts (**B**). In contrast to *Hesr1*, *Hesr2* is expressed in the ventricle in wild-type hearts (**D**) and its distribution is not altered in NICD1-activated hearts (**E**). Abbreviations: LA, left atrium; RA, right atrium; LV, left ventricle; RA, right ventricle. Scale bar: 500 μm in E.

Hence, if the defects in NICD1-activated hearts were due to the suppression of specific genes by elevated *Hesr1*, we would expect that they would be rescued by the absence of Hesr1. Unexpectedly, however, most of defects observed in NICD1-activated hearts were also elicited by Notch1 activation, even in the absence of *Hesr1* (Fig. 5A-D, Fig. 1A-D). In the NICD1-activated/*Hesr1*-null hearts, impaired ventricular trabeculation and cell masses in the cushion tissue (Fig. 5F, arrowhead) were again observed, as seen in NICD1-activated hearts (Fig. 2B). However, we observed that there was much less trabeculation of the AV myocardium in the NICD1-activated/*Hesr1*-null background, suggesting that the property of the AV myocardium is recovered (Fig. 5F, brackets), whereas the IVS was again right-shifted (Fig. 5F, arrow). These data indicate that ectopic *Hesr1* expression in the myocardium may have caused the defects observed in the AV myocardium.

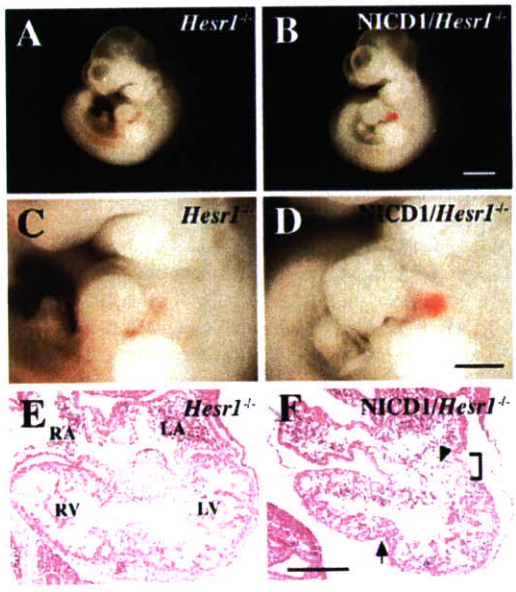

Fig. 5. NICD1-activated hearts in a *Hesr1*-null background at E10.5. *Hesr1*-null mice do not show any detectable defects (**A**,**C**,**E**) and NICD1-activation in *Hesr1*-null induced heart defects (**B**,**D**) is similar to NICD-activation in Hesr1-positive mice. Hematoxylin and Eosin analysis also revealed impaired trabeculation, the appearance of cell masses in the AV cushion (arrowhead) and a right-shifted interventricular septum (arrow). However, the AV myocardium is recovered (brackets) (**F**). Abbreviations: LA, left atrium; RA, right atrium; LV, left ventricle; RA, right ventricle. Scale bar: 1 mm in B; 500 μm in D; 200 μm in F.

Wnt2, *Bmp6*, *Tnni2* and *Jag1* are induced in NICD1-activated hearts

As it was unlikely that Hesr1 would be the sole mediator of Notch1 signaling, and because Hesr1-independent mechanisms must be involved in the formation of the defects in NICD1-activated hearts, we examined the expression of several genes that could potentially be involved in these myocardial abnormalities. However, following RT-PCR experiments, we could not find any critical changes in the expression levels of the genes that we selected for analysis (*Mlc2a*, *Mlc2v*, *Mhca*, *Mhcb*, *Nkx2.5*, *Mef2c*, *Gata4*, *Nrg1*, *Erbb4*, *Ccnd1*, *Jmj*, *Snail*) (Supplementary Fig. S1). Therefore, to identify candidate genes that are differentially regulated in NICD1-activated hearts, we performed comparative GeneChip analysis using RNA isolates from ventricles with an AV canal from transgenic and wild-type hearts at E10.5. These experiments identified several genes showing differences in their expression levels between wild-type and NICD1-activated mice. Since we had observed that the lack of Hesr1, which is known to function as a transcriptional suppressor (Iso et al., 2001b), only rescues the AV myocardium, we focused on genes that were upregulated in NICD1-activated hearts (see Table S1 in the supplementary material). Among the candidates that we analyzed were *Wnt2*, *Bmp6* and troponin 1 fast-twitch skeletal muscle isoform (*Tnni2*), which we subsequently confirmed by RT-PCR and in situ hybridization (Fig. 6). In wild-type hearts, *Wnt2* is expressed strongly in the posterior region, e.g. the sinus venosus (Monkley et al., 1996) and the atrium, but it is difficult to detect its expression in the ventricle of wild-type hearts (Fig. 6B,B′). However, *Wnt2* expression was easily detectable in NICD1-activated hearts (Fig. 6C). Transverse sections also revealed stronger ectopic expression of *Wnt2* in the left ventricle, including the AV canal (Fig. 6C′).

Similar expression changes was observed for *Bmp6* (Fig. 6D-E′), which is normally expressed in the OFT and cushion tissue (Kim et al., 2001b). In wild-type hearts, *Tnni2* expression was found to be marginally expressed in the atrium (Fig. 6F,F′), but to be strongly induced both in the atria and the ventricles in NICD1-activated hearts (Fig. 6G,G′). Tnni2 is one of the components of troponin 1, and is known to inhibit the interaction between actin and myosin in the absence of Ca^{2+} (Clark et al., 2002; Gordon et al., 2000). Hence, the elevated expression of *Tnni2* might be one of the leading causes of the induction of the myocardial structural defects in NICD1-activated mice. We observed that one of the known Notch ligands,

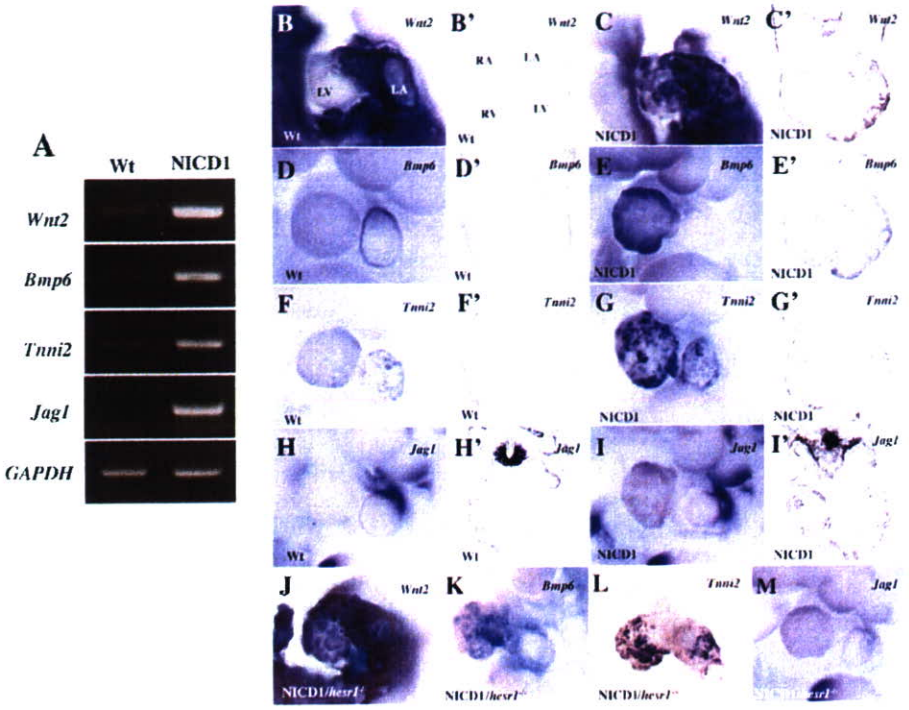

Fig. 6. Upregulation of *Wnt2*, *Bmp6*, *Tnni2* and *Jag1* in NICD1-activated hearts at E10.5. (**A**) RT-PCR analysis was performed using RNA from the ventricle with the AV canal. Expression of *Wnt2*, *Bmp6*, *Tnni2* and *Jag1* is upregulated in NICD1-activated hearts. (**B-I'**) Whole-mount and section in situ hybridization confirmed the upregulation of these genes (B,B',D,D',F,F',H,H', wild-type hearts; C,C',E,E',G,G',I,I', NICD1-activated hearts). The upregulation is also observed in NICD1-activated hearts in a *Hesr1*-null background (**J-M**). Abbreviations: LA, left atrium; RA, right atrium; LV, left ventricle; RA, right ventricle.

Jag1, is also induced in NICD1-activated hearts (Fig. 6A). *Jag1* is expressed in the atria, right ventricle and OFT of wild-type hearts (Fig. 6H,H'), and this expression was found to be expanded into the whole heart in NICD1-activated mice (Fig. 6I,I'). We also examined the distribution of these genes at E8.5 to determine whether their expression profiles are affected from an earlier stage. Although the upregulation of NICD1 expression was not clear in the NICD1-activated hearts at this stage (see Fig. S4A,B in the supplementary material), we observed increased expression of the above genes and also morphological changes (rough surface) in NICD1-activated hearts (see Fig. S4D,F,H,J in the supplementary material).

As all of these expression changes coincide with the *Hesr1* expression pattern, we speculated that they are in fact the result of secondary effects of Hesr1 induction. To address this possibility, we examined the expression of each of these genes in the NICD1-activated hearts of Hesr1 knockout mice. As shown in Fig. 6J-M, elevated gene expression was observed for *Wnt2*, *Bmp6*, *Tnni2* and *Jag1*, even in the absence of Hesr1. These data indicate that the activation of these genes is either mediated by a factor other than Hesr1 or is directly regulated by NICD1.

DISCUSSION

In this study, we have generated NICD1-activated mice and analyzed their cardiac lineage. NICD1-activated hearts showed abnormal morphologies, such as disrupted cardiomyocyte differentiation, the appearance of ectopic cell masses in the AV cushion, a right-shifted IVS and defects in the AV myocardium. Moreover, these NICD1-activated mice died at E10.5. It has been shown that the AV myocardium is important for connection formation between the right atrium and right ventricle, and the left atrium and left ventricle at the end of looping (Kim et al., 2001a). Furthermore, it has been suggested that the AV node develops from that part of the AV canal myocardium. Therefore, we speculate that the transgenic embryo does not form a complete heart with normal cardiac morphology and conduction system, resulting in death at an early stage. Comparisons with NICD1-activated hearts in a *Hesr1*-null background demonstrate that ectopic *Hesr1* expression is responsible for the differentiation of the AV myocardium. In NICD1-activated hearts, the expression of *Wnt2*, *Bmp6*, *Tnni2* and *Jag1* could be induced in addition to *Hesr1*, and this might well be the cause of these myocardial abnormalities.

The involvement of Notch signaling in cardiac cell fates

In *Xenopus*, the expression of *Serrate1* (*Xenopus Jag1*) and *Notch1* overlaps in the dorsal side of the heart, and the forced expression of the activated form of Su(H) (*Xenopus* RBPjκ) suppresses the expression of myocardial genes (Rones et al., 2000). This indicates that Jag1-Notch1 signaling in *Xenopus* has an inhibitory effect upon myocardial fate determination. Although the expression levels of myocardial genes were shown previously not to change in either NICD1-activated, *Notch1* or *Rbpsuh* mutant hearts (Timmerman et al., 2004), our current histological data suggests that Notch1 signaling suppresses myocardial differentiation but does not affect myocardial cell fate decisions. In addition, the ectopic expression of Su(H) in *Xenopus* embryos results in the reduction of the number of myocardial cells that contribute to the heart (Rones et al., 2000). In the mouse, by contrast, abnormal trabeculation of the AV myocardium was observed in NICD1-activated hearts and this defect was rescued by a lack of Hesr1, which indicates that Notch/Hesr1 signaling might have suppressive effects for AV myocardial differentiation in the mouse.

The suppressive effects of Notch1 signaling on cardiomyocyte maturation

We observed the suppression of myocardial differentiation in NICD1-activated hearts and confirmed the presence of myofibrillar disorganization in their trabeculae by TEM analyses. Notch1

signaling in the wild-type mouse heart is restricted to the endocardial cells, as we observe Notch1 activation by antibody staining only in the endocardium. In NICD1-activated hearts, however, Notch1 signaling is also activated in the myocardium. Therefore, it is likely that the ectopic Notch1 activation in myocardium may directly suppresses differentiation, but it is also possible that secreted factor(s) from the endocardium (Bmp6 and Wnt2 are the candidates), that might be activated by additional NICD1, negatively regulate cardiomyocyte differentiation. If this is indeed the case, we speculate that Notch1 signaling negatively regulates cardiomyocyte differentiation. However, the effects of Notch1/Rbpsuh signaling upon myocardial development are not fully clear because heart formation itself is severely retarded in *Rbpsuh*-null mutants (Timmerman et al., 2004). We also have investigated conditional knockout embryos for the *Rbpsuh* allele driven by *Mesp1-Cre*. However, the resulting phenotype was similar to that of the *Rbpsuh*-null embryo and the heart was underdeveloped (data not shown), possibly owing to the early onset of *Mesp1*.

The role of Notch1 signaling in the AV myocardium

In our current experiments, Mhc, αSma-positive and Pecam-negative cell masses were observed in the AV cushion of NICD1-activated hearts. From our observations of serial sections of NICD1-activated hearts, we postulate that these cell masses could originate from the AV myocardium, where trabeculation is normally prevented in the wild-type AV canal. Bmp2 is a crucial factor in the determination of AV myocardial identity by regulating *Tbx2* and its downstream genes, including *Anf* and *Smpx* (Ma et al., 2005). In the NICD1-activated heart, the decreased expression of *Bmp2* and *Tbx2* in the AV myocardium should cause the loss of an AV identity, which in turn might confer the chamber identity to the AV canal, as evidenced by ambiguous *Anf* and *Smpx* expression. This may also induce ectopic trabeculation in the AV myocardium. The other possibility that we have considered for the origins of the cell masses are the endocardial cells. This is based upon the severe defects that can be observed in endocardial development and EMT in both *Notch1* and *Rbpsuh*-null mice (Timmerman et al., 2004). Furthermore, it has been reported that Notch1 activation induces the transformation of either AV canal explants or endothelial cells to αSma-positive cells (Noseda et al., 2004; Timmerman et al., 2004). Although it is not clear whether these transformed cells also express Mhc, the cell masses in the NICD1-activated AV cushion might well be derived from endocardial cells due to excess EMT.

Implications of the upregulated genes identified in NICD1-activated mouse hearts

In vitro experiments have indicated that both *Hesr1* and *Hesr2* are induced by NICD1 (Iso et al., 2002; Iso et al., 2001a; Nakagawa et al., 2000). However, in NICD1-activated hearts, *Hesr1* was strongly induced but not *Hesr2*, suggesting that the regulatory mechanism is different between these genes. A possible function for the Hes proteins in these events, as they are also induced in NICD1-activated hearts, will need to be addressed in future studies.

In addition to Hes family genes, we have found that many genes are induced in NICD1-activated hearts. Among these, the upregulation of *Tnni2* might be responsible for the observed myocardial defects. In the mouse heart, the most abundant troponin 1 is *Tnni3* (cardiac *Tnni*), but *Tnni2* is also transiently expressed in embryonic hearts from E9.5 to E16.5 (Zhu et al., 1995). *Tnni2* mutant mice have not been reported, but *Tnni3* mutant mice have been generated and show shortened sarcomere lengths (Huang et al., 1999). A single *Tnni* gene has been identified in *Drosophila*; its mutant, *hdp*^{3}, exhibits impaired sarcomere structure (Nongthomba et al., 2004). The strong induction of *Tnni2* by NICD1 may therefore be one of main causes of the disrupted sarcomere structure in NICD1-activated hearts. *Wnt2* is normally expressed in early cardiac mesoderm and thereafter in the sinus venosus and OFT regions (Monkley et al., 1996). However, signals detected using a LEF/TCF reporter (TOPGal) did not differ between wild-type and NICD1-activated hearts (see Fig. S5 in the supplementary material), which suggests that Wnt2 uses a non-canonical Wnt pathway in the mouse heart. Recently, it has been shown that a non-canonical Wnt11 signaling pathway is crucial for cardiogenesis and cardiomyocyte differentiation (Pandur et al., 2002; Terami et al., 2004), and that its expression pattern overlaps in the OFT with Wnt2. These non-canonical Wnt signaling mechanisms must therefore be involved in cardiogenesis.

We also demonstrate in our current experiments that there is a strong induction of *Bmp6* by Notch1 signaling. The importance of BMP6 signaling during cardiac development was previously reported by the analysis of *Bmp6/Bmp7* double-null mice, which showed retarded OFT cushion development, reduced trabeculation and failure of septation (Kim et al., 2001b), although single mutations of *Bmp6* or *Bmp7* did not induce any defects in the heart (Dudley et al., 1995; Luo et al., 1995; Solloway et al., 1998). As Bmp signaling inhibits myogenic differentiation synergistically with Notch1 signaling in C2C12 cells (Dahlqvist et al., 2003), this synergistic effect might lead to the suppression of myocardial differentiation in NICD1-activated ventricles.

Although NICD1 is activated in both sides (left and right) of the atrium and ventricle in the NICD1-activated heart, the strong induction of *Wnt2* and *Bmp6* was restricted to the left ventricle, whereas *Tnni2* and *Jag1* are induced in both sides of the ventricle. The reason for the restriction of *Wnt2* and *Bmp6* is currently unknown, but it may suggest the different responsiveness between the left and right ventricles to NICD1. The upregulation of these genes in NICD1-activated hearts was not mediated by Hesr1 and therefore might be regulated by direct binding of Rbpsuh to the enhancer region or by other Hes genes. Multiple putative binding sites for Su (H) (Rbpsuh) (more than 80% homology to consensus sequence) and also Hairy-binding sites (N-box sites) are present within the 10 kb upstream and downstream flanking regions of the *Wnt2*, *Bmp6*, *Tnni2* and *Jag1* transcription start sites (TFSEARCH; http://mbs.cbrc.jp/research/db/TFSEARCH.html). However, further enhancer analyses will be required to determine their functional relevance.

Our present study was initially designed to further understand the function of Notch signaling during cell fate decisions by ectopically expressing activated Notch1 in their precursors. Although we did not observe any cell fate changes during cardiac development, our detailed analyses of transgenic mouse phenotypes and downstream target genes enabled us to uncover several important aspects of Notch signaling in cardiac development. The functional differences between Hesr1 and Hesr2 are now of great interest in these events, and understanding the crosstalk between Notch and other signaling pathways, such as Wnt or Bmp, are obviously crucial for correct heart development. Further studies using gain- or loss-of-function experiments will now be required to fully elucidate the molecular mechanisms underlying cardiac development in the mouse.

We are grateful to Dr Hiroaki Nagao for the electron microscopic analysis, to Dr Satoshi Kitajima for helpful advice and discussions about Microarray analysis, and to the *Mesp1*-lineage experiments and Dr Tasuku Honjo for generously providing the *Rbpsuh* mutant mice. We would also like to

acknowledge our colleagues who provided us with cDNAs for use as probes, including Drs R. A. Conlon (*Notch1*), T. A. Mitsiadis (*Jag1*), I. Satokata (*Anf*), M. Shirai (*Tbx2*), M. E. Dickinson (*Bmp2*) and T. Takeuchi (*Hand1*). We also thank Ms Yuki Takahashi and Ms Yuka Sato for technical assistance, and Mr Okamura and Mr Oginuma for their support. This work was supported by the Organized Research Combination System and National BioResource Project of the Ministry of Education, Culture, Sports, Science and Technology, Japan.

Supplementary material

Supplementary material for this article is available at http://dev.biologists.org/cgi/content/full/133/9/1625/DC1

References

Artavanis-Tsakonas, S., Rand, M. D. and Lake, R. J. (1999). Notch signaling: cell fate control and signal integration in development. *Science* **284**, 770-776.

Buckingham, M., Meilhac, S. and Zaffran, S. (2005). Building the mammalian heart from two sources of myocardial cells. *Nat. Rev. Genet.* **6**, 826-835.

Clark, K. A., McElhinny, A. S., Beckerle, M. C. and Gregorio, C. C. (2002). Striated muscle cytoarchitecture: an intricate web of form and function. *Annu. Rev. Cell Dev. Biol.* **18**, 637-706.

Dahlqvist, C., Blokzijl, A., Chapman, G., Falk, A., Dannaeus, K., Ibanez, C. F. and Lendahl, U. (2003). Functional Notch signaling is required for BMP4-induced inhibition of myogenic differentiation. *Development* **130**, 6089-6099.

de la Cruz, M. and Miller, B. (1968). Double-inlet ventricle: two pathological speciments with comments on the embryology alid on its relation to single ventricle. *Circulation* **37**, 249-260.

Donovan, J., Kordylewska, A., Jan, Y. N. and Utset, M. F. (2002). Tetralogy of fallot and other congenital heart defects in Hey2 mutant mice. *Curr. Biol.* **12**, 1605-1610.

Dudley, A. T., Lyons, K. M. and Robertson, E. J. (1995). A requirement for bone morphogenetic protein-7 during development of the mammalian kidney and eye. *Genes Dev.* **9**, 2795-2807.

Fischer, A., Schumacher, N., Maier, M., Sendtner, M. and Gessler, M. (2004). The Notch target genes Hey1 and Hey2 are required for embryonic vascular development. *Genes Dev.* **18**, 901-911.

Garg, V., Muth, A. N., Ransom, J. F., Schluterman, M. K., Barnes, R., King, I. N., Grossfeld, P. D. and Srivastava, D. (2005). Mutations in NOTCH1 cause aortic valve disease. *Nature* **437**, 270-274.

Gessler, M., Knobeloch, K. P., Helisch, A., Amann, K., Schumacher, N., Rohde, E., Fischer, A. and Leimeister, C. (2002). Mouse gridlock: no aortic coarctation or deficiency, but fatal cardiac defects in *Hey2*$^{-/-}$ mice. *Curr. Biol.* **12**, 1601-1604.

Gordon, A. M., Homsher, E. and Regnier, M. (2000). Regulation of contraction in striated muscle. *Physiol. Rev.* **80**, 853-924.

Hamada, Y., Kadokawa, Y., Okabe, M., Ikawa, M., Coleman, J. R. and Tsujimoto, Y. (1999). Mutation in ankyrin repeats of the mouse Notch2 gene induces early embryonic lethality. *Development* **126**, 3415-3424.

Han, Z. and Bodmer, R. (2003). Myogenic cells fates are antagonized by Notch only in asymmetric lineages of the Drosophila heart, with or without cell division. *Development* **130**, 3039-3051.

Huang, X., Pi, Y., Lee, K. J., Henkel, A. S., Gregg, R. G., Powers, P. A. and Walker, J. W. (1999). Cardiac troponin I gene knockout: a mouse model of myocardial troponin I deficiency. *Circ. Res.* **84**, 1-8.

Iso, T., Sartorelli, V., Chung, G., Shichinohe, T., Kedes, L. and Hamamori, Y. (2001a). HERP, a new primary target of Notch regulated by ligand binding. *Mol. Cell. Biol.* **21**, 6071-6079.

Iso, T., Sartorelli, V., Poizat, C., Iezzi, S., Wu, H. Y., Chung, G., Kedes, L. and Hamamori, Y. (2001b). HERP, a novel heterodimer partner of HES/E(spl) in Notch signaling. *Mol. Cell. Biol.* **21**, 6080-6089.

Iso, T., Chung, G., Hamamori, Y. and Kedes, L. (2002). HERP1 is a cell type-specific primary target of Notch. *J. Biol. Chem.* **277**, 6598-6607.

Iso, T., Kedes, L. and Hamamori, Y. (2003). HES and HERP families: multiple effectors of the Notch signaling pathway. *J. Cell Physiol.* **194**, 237-255.

Kaneta, M., Osawa, M., Sudo, K., Nakauchi, H., Farr, A. G. and Takahama, Y. (2000). A role for pref-1 and HES-1 in thymocyte development. *J. Immunol.* **164**, 256-264.

Kim, J. S., Viragh, S., Moorman, A. F., Anderson, R. H. and Lamers, W. H. (2001a). Development of the myocardium of the atrioventricular canal and the vestibular spine in the human heart. *Circ. Res.* **88**, 395-402.

Kim, R. Y., Robertson, E. J. and Solloway, M. J. (2001b). Bmp6 and Bmp7 are required for cushion formation and septation in the developing mouse heart. *Dev. Biol.* **235**, 449-466.

Kitajima, S., Miyagawa-Tomita, S., Inoue, T., Kanno, J. and Saga, Y. (2006). Mesp1-nonexpressing cells contribute to the ventricular cardiac conduction system. *Dev. Dyn.* **235**, 395-402.

Kokubo, H., Miyagawa-Tomita, S., Tomimatsu, H., Nakashima, Y., Nakazawa, M., Saga, Y. and Johnson, R. L. (2004). Targeted disruption of hesr2 results in atrioventricular valve anomalies that lead to heart dysfunction. *Circ. Res.* **95**, 540-547.

Kokubo, H., Miyagawa-Tomita, S., Nakazawa, M., Saga, Y. and Johnson, R. L. (2005). Mouse hesr1 and hesr2 genes are redundantly required to mediate Notch signaling in the developing cardiovascular system. *Dev. Biol.* **278**, 301-309.

Leimeister, C., Externbrink, A., Klamt, B. and Gessler, M. (1999). Hey genes: a novel subfamily of hairy- and Enhancer of split related genes specifically expressed during mouse embryogenesis. *Mech. Dev.* **85**, 173-177.

Luo, G., Hofmann, C., Bronckers, A. L., Sohocki, M., Bradley, A. and Karsenty, G. (1995). BMP-7 is an inducer of nephrogenesis, and is also required for eye development and skeletal patterning. *Genes Dev.* **9**, 2808-2820.

Ma, L., Lu, M. F., Schwartz, R. J. and Martin, J. F. (2005). Bmp2 is essential for cardiac cushion epithelial-mesenchymal transition and myocardial patterning. *Development* **132**, 5601-5611.

McCright, B., Lozier, J. and Gridley, T. (2002). A mouse model of Alagille syndrome: Notch2 as a genetic modifier of Jag1 haploinsufficiency. *Development* **129**, 1075-1082.

Miyagawa-Tomita, S., Morishima, M., Nakazawa, M., Mizutani, M. and Kikuchi, T. (1996). Pathological study of Japanese quail embryo with acid alpha-glucosidase deficiency during early development. *Acta Neuropathol. (Berl)* **92**, 249-254.

Monkley, S. J., Delaney, S. J., Pennisi, D. J., Christiansen, J. H. and Wainwright, B. J. (1996). Targeted disruption of the Wnt2 gene results in placentation defects. *Development* **122**, 3343-3353.

Nakagawa, O., Nakagawa, M., Richardson, J. A., Olson, E. N. and Srivastava, D. (1999). HRT1, HRT2, and HRT3: a new subclass of bHLH transcription factors marking specific cardiac, somitic, and pharyngeal arch segments. *Dev. Biol.* **216**, 72-84.

Nakagawa, O., McFadden, D. G., Nakagawa, M., Yanagisawa, H., Hu, T., Srivastava, D. and Olson, E. N. (2000). Members of the HRT family of basic helix-loop-helix proteins act as transcriptional repressors downstream of Notch signaling. *Proc. Natl. Acad. Sci. USA* **97**, 13655-13660.

Neuhaus, H., Rosen, V. and Thies, R. S. (1999). Heart specific expression of mouse BMP-10 a novel member of the TGF-beta superfamily. *Mech. Dev.* **80**, 181-184.

Nongthomba, U., Clark, S., Cummins, M., Ansari, M., Stark, M. and Sparrow, J. C. (2004). Troponin I is required for myofibrillogenesis and sarcomere formation in Drosophila flight muscle. *J. Cell Sci.* **117**, 1795-1805.

Noseda, M., McLean, G., Niessen, K., Chang, L., Pollet, I., Montpetit, R., Shahidi, R., Dorovini-Zis, K., Li, L., Beckstead, B. et al. (2004). Notch activation results in phenotypic and functional changes consistent with endothelial-to-mesenchymal transformation. *Circ. Res.* **94**, 910-917.

Pandur, P., Lasche, M., Eisenberg, L. M. and Kuhl, M. (2002). Wnt-11 activation of a non-canonical Wnt signalling pathway is required for cardiogenesis. *Nature* **418**, 636-641.

Park, M., Yaich, L. E. and Bodmer, R. (1998). Mesodermal cell fate decisions in Drosophila are under the control of the lineage genes numb, Notch, and sanpodo. *Mech. Dev.* **75**, 117-126.

Reaume, A. G., Conlon, R. A., Zirngibl, R., Yamaguchi, T. P. and Rossant, J. (1992). Expression analysis of a Notch homologue in the mouse embryo. *Dev. Biol.* **154**, 377-387.

Rones, M. S., McLaughlin, K. A., Raffin, M. and Mercola, M. (2000). Serrate and Notch specify cell fates in the heart field by suppressing cardiomyogenesis. *Development* **127**, 3865-3876.

Saga, Y., Miyagawa-Tomita, S., Takagi, A., Kitajima, S., Miyazaki, J. and Inoue, T. (1999). MesP1 is expressed in the heart precursor cells and required for the formation of a single heart tube. *Development* **126**, 3437-3447.

Saga, Y., Kitajima, S. and Miyagawa-Tomita, S. (2000). Mesp1 expression is the earliest sign of cardiovascular development. *Trends Cardiovasc. Med.* **10**, 345-352.

Sakata, Y., Kamei, C. N., Nakagami, H., Bronson, R., Liao, J. K. and Chin, M. T. (2002). Ventricular septal defect and cardiomyopathy in mice lacking the transcription factor CHF1/Hey2. *Proc. Natl. Acad. Sci. USA* **99**, 16197-16202.

Schroeder, T., Fraser, S. T., Ogawa, M., Nishikawa, S., Oka, C., Bornkamm, G. W., Honjo, T. and Just, U. (2003). Recombination signal sequence-binding protein Jkappa alters mesodermal cell fate decisions by suppressing cardiomyogenesis. *Proc. Natl. Acad. Sci. USA* **100**, 4018-4023.

Shirayoshi, Y., Yuasa, Y., Suzuki, T., Sugaya, K., Kawase, E., Ikemura, T. and Nakatsuji, N. (1997). Proto-oncogene of int-3, a mouse Notch homologue, is expressed in endothelial cells during early embryogenesis. *Genes Cells* **2**, 213-224.

Solloway, M. J., Dudley, A. T., Bikoff, E. K., Lyons, K. M., Hogan, B. L. and Robertson, E. J. (1998). Mice lacking Bmp6 function. *Dev. Genet.* **22**, 321-339.

Takahashi, Y., Koizumi, K., Takagi, A., Kitajima, S., Inoue, T., Koseki, H. and Saga, Y. (2000). Mesp2 initiates somite segmentation through the Notch signalling pathway. *Nat. Genet.* **25**, 390-396.

Terami, H., Hidaka, K., Katsumata, T., Iio, A. and Morisaki, T. (2004). Wnt11 facilitates embryonic stem cell differentiation to Nkx2.5-positive cardiomyocytes. *Biochem. Biophys. Res. Commun.* **325**, 968-975.

Timmerman, L. A., Grego-Bessa, J., Raya, A., Bertran, E., Perez-Pomares, J. M., Diez, J., Aranda, S., Palomo, S., McCormick, F., Izpisua-Belmonte, J. C.

et al. (2004). Notch promotes epithelial-mesenchymal transition during cardiac development and oncogenic transformation. *Genes Dev.* **18**, 99-115.
Wenink, A. C. (1981). Embryology of the ventricular septum. Separate origin of its components. *Virchows Arch. A Pathol. Anat. Histol.* **390**, 71-79.
Williams, R., Lendahl, U. and Lardelli, M. (1995). Complementary and combinatorial patterns of Notch gene family expression during early mouse development. *Mech. Dev.* **53**, 357-368.
Yamauchi, Y., Abe, K., Mantani, A., Hitoshi, Y., Suzuki, M., Osuzu, F., Kuratani, S. and Yamamura, K. (1999). A novel transgenic technique that allows specific marking of the neural crest cell lineage in mice. *Dev. Biol.* **212**, 191-203.
Zhu, L., Lyons, G. E., Juhasz, O., Joya, J. E., Hardeman, E. C. and Wade, R. (1995). Developmental regulation of troponin I isoform genes in striated muscles of transgenic mice. *Dev. Biol.* **169**, 487-503.

Journal of Pathology
J Pathol 2006; **209**: 522–531
Published online 25 April 2006 in Wiley InterScience (www.interscience.wiley.com). **DOI:** 10.1002/path.1993

Original Paper

PTOV1: a novel testosterone-induced atherogenic gene in human aorta

Y Nakamura,[1] T Suzuki,[1] K Igarashi,[4] J Kanno,[4] T Furukawa,[2] C Tazawa,[1] F Fujishima,[1] I Miura,[1] T Ando,[4] N Moriyama,[1] T Moriya,[1] H Saito,[5] S Yamada[3] and H Sasano[1]*

[1]*Department of Pathology, Tohoku University School of Medicine, Sendai, Japan*
[2]*Department of Molecular Pathology, Tohoku University School of Medicine, Sendai, Japan*
[3]*Department of Radiology, Tohoku University School of Medicine, Sendai, Japan*
[4]*Division of Toxicology, the Biological Safety Research Centre, National Institute of Health Sciences, Tokyo, Japan*
[5]*Department of Radiology, Sendai Medical Centre, Sendai, Japan*

*Correspondence to:
Dr H Sasano, Department of Pathology, Tohoku University School of Medicine, 2-1 Seiryo-machi, Aoba-ku, Sendai, 980-8575 Japan.
E-mail: hsasano@patholo2.med.tohoku.ac.jp

Received: 25 October 2005
Revised: 8 February 2006
Accepted: 4 March 2006

Abstract

There are gender differences in the development of atherosclerosis, possibly owing to differences in sex steroid hormone action and/or metabolism. One of the atherogenic effects of testosterone is thought to be androgen receptor (AR)-mediated vascular smooth muscle cell (VSMC) proliferation. However, the detailed mechanism of this effect, particularly the identity of the genes associated with VSMC proliferation, remains largely unknown. Therefore, we first employed microarray analysis and, subsequently, quantitative RT-PCR to analyse RNA expression in AR-positive human VSMCs treated with testosterone in order to detect testosterone-induced genes associated with cell proliferation. We further examined whether the genes identified were involved in cell proliferation using small interfering RNA (siRNA) transfection. Expression of the gene products was then evaluated in human aorta with various degrees of atherosclerosis in order to evaluate the clinical relevance of the findings. Both microarray and quantitative RT-PCR analyses demonstrated marked induction of the human prostate overexpressed protein 1 (*PTOV1*) gene by testosterone in the cell lines: this gene was recently identified as a novel androgen-induced gene involved in prostate tumour cell proliferation. Inhibition of *PTOV1* by transfection of its corresponding siRNA suppressed testosterone-induced cell proliferation. In human aorta, PTOV1 immunoreactivity in the nuclei of neointimal VSMCs was abundantly detected in male aorta with mild atherosclerotic changes compared with female aorta or male aorta with severe atherosclerotic changes. These findings indicate that the *PTOV1* gene is androgen-responsive in VSMCs and that it may play an important role in androgen-related atherogenesis in the human aorta, particularly early atherosclerosis in the male aorta, through regulating proliferation of neointimal VSMCs.

Keywords: vascular smooth muscle cells; androgen receptor; testosterone; cell proliferation; PTOV1

Introduction

There is an important, well-documented, gender difference in coronary heart disease risks, with earlier onset of disease and excess mortality in male subjects [1–3]. Athero-protective effects of oestrogens on vascular structure and function have been proposed as one of the most important mechanisms accounting for this gender difference [4]. On the other hand, an association between androgens and atherosclerosis continues to be disputed. Androgens have been considered to reduce the incidence of ischaemic myocardial disease in men, but they have also been reported to exert atherogenic effects on the human cardiovascular system through promoting plaque formation and enhancing monocyte adhesion to endothelial cells [5–8]. It has been demonstrated that testosterone exerts direct atherogenic effects by promoting cell proliferation through an initial interaction with the androgen receptor (AR) in vascular smooth muscle cells (VSMCs) *in vitro* [9]. However, unlike oestrogens, the possible effects of testosterone on atherogenesis and/or anti-atherogenesis have not been extensively studied. It is therefore important to study the detailed mechanisms of these direct effects of testosterone on the human cardiovascular system.

In this study, we first screened for testosterone-induced genes involved in the proliferation of VSMCs using microarray analysis in cell lines derived from AR-positive human VSMCs. We then confirmed the results by employing other *in vitro* studies. As testosterone induced marked overexpression of *PTOV1* in

these assays, we subsequently examined the levels of expression of PTOV1 protein in VSMCs in samples of the human abdominal aorta obtained at autopsy.

Materials and methods

Vascular smooth muscle cells

Two types of human dedifferentiated VSMCs, ie HUVS-112D (derived from human umbilical cord), and T/G HA-VSMC (derived from human aorta) were commercially obtained from American Type Culture Collection (Manassas, VA, USA) [10,11]. We examined whether these cells expressed AR using an RT/real-time PCR with a light Cycler System using DNA binding dye SYBR Green I, and immunoblotting with AR polyclonal antibody (Santa Cruz Biotechnology, Inc, Santa Cruz, CA, USA), as reported previously [10,12].

GeneChip microarray assay

The VSMCs above were cultured until a sub-confluent state was achieved. The medium was then replaced with fetal bovine serum (FBS)-free and phenol red-free medium to arrest cell proliferation. After 24 h, the medium was replaced again with phenol red-free and FBS-free medium in the presence of testosterone (10 nM) or vehicle (0.1% ethanol). After incubation for 2 h, the cells were subsequently subjected to total RNA extraction for microarray analysis. Isolated total RNA was labelled as described in the Affymetrix (Santa Clara, CA, USA) GeneChip Expression Analysis Technical Manual (revision 3), as previously described [10]. The ratios represent the values up- or down-regulated by 10 nM testosterone treatment compared with control. We independently repeated the same experiment twice. Genes for which the average ratios increased more than 1.5-fold in both experiments using 10 nM testosterone treatment were considered up-regulated via AR when compared with control values [13]. When studying the potential functions of these genes, we used the homepage of the HUGO Gene Nomenclature Committee (http://www.gene.ucl.ac.uk/nomenclature, accessed 28 March 2006) for further examination of whether any had been previously reported to be involved in cell proliferation and to be associated with androgen effects. In this study, among the genes that were found to be significantly induced by testosterone treatment by microarray analysis, we regarded a gene that was up-regulated, and was known to be associated with both cell proliferation and androgenic effects, as a target gene.

Quantitative real-time PCR

After achieving sub-confluence and following growth arrest states of the VSMCs as described above, the medium was replaced again with phenol red-free and FBS-free F12-K medium with testosterone (10 nM), testosterone (10 nM) with flutamide, an AR-blocker (100 nM), or vehicle. After incubation for 2 h, the cells were subsequently subjected to total RNA extraction for RT/real-time PCR analysis, described previously [10]. mRNA levels for the target gene *PTOV1* were determined in each VSMC as a ratio relative to glyceraldehyde-3-phosphate dehydrogenase (*GAPDH*), and evaluated as a ratio (%) compared with that of each control cDNA. The analyses with real-time PCR were repeated three times. Table 1 summarizes the primers used [14].

siRNA preparation, transfection, and cell count assay

Small interfering RNAs (siRNAs) corresponding to *PTOV1* (Table 2) were synthesized based on results of a previous report, and were transfected into the VSMCs [15]. These VSMCs were seeded in a 24-well plate at an initial concentration of 50 000 cells/well with F-12K medium containing 2% FBS and were cultured until a sub-confluent status was achieved. The medium was then replaced with phenol red-free and FBS-free medium to arrest cell proliferation. After 24 h, transfection experiments of siRNA for endogenous gene targeting (10 nM or 100 nM) were carried out using RNAiFect™ transfection reagent (Qiagen, Valencia, CA, USA). After transfection, the cells were incubated in phenol red-free medium containing 2% dextran-coated, charcoal-stripped FBS with testosterone (10 nM) or vehicle (0.1% ethanol) for 24 h. We measured the number of cells in each sample as described above with Cell Counting Kit-8 system (Wako, Tokyo, Japan) after incubation for 48 h. We also examined the number of cells treated with

Table 1. Primer sequences used in RT-PCR analysis

cDNA	Sequence	Size (bp)
AR	Forward 5′-CTCACCAAGCTCCTGGACTC-3′ Reverse 5′-CAGGCAGAAGACATCTGAAG-3′	246
GAPDH	Forward 5′-TGAACGGGAAGCTCACTGG-3′ Reverse 5′-TCCACCACCCTGTTGCTGTA-3′	307
PTOV1	Forward 5′-CACCATCCCTCCATGTTGCTG-3′ Reverse 5′-TCTTCATTGGCCTCATCCCC-3′	250

Table 2. Sequences used in siRNA transfection analysis

cDNA	Sequence
PTOV1	Sense r(CAACAAGUUUCUGGCAUGG)dTdT Antisense r(CCAUGCCAGAAACUUGUUG)dTdT
Negative control	Sense r(UUCUCCGAACGUGUCACGU)dTdT Antisense r(ACGUGACACGUUCGGAGAA)dTdT

The target gene in this study (*PTOV1*) was determined by microarray analysis. The sequences of *PTOV1* siRNAs are based on a previous report [15].

transfection of negative control siRNA with scrambled sequences (Table 2), and treated with testosterone (10 nM) or vehicle. In order to evaluate transfection efficiency, we examined relative *PTOV1* mRNAs levels in these cells at 24 h after transfection of the specific siRNAs. The mRNA levels in each VSMC were calculated as a ratio relative to *GAPDH*, and were normalized to the ratio after transfection of negative control siRNA (10 nM).

Quantitative RT-PCR analysis of *PTOV1* mRNA expression in human aorta

Samples of human abdominal aorta were collected at autopsy from patients without a history of hormone replacement therapy. Autopsies were performed on 32 subjects (16 male, 16 female; mean 60.7 ± 3.3 years) in Tohoku University Hospital (Sendai, Japan) within 2 h post mortem. The Ethics Committee at Tohoku University School of Medicine approved the research protocol for this study. Aortic specimens were tentatively classified into the following four groups according to the sex of the deceased patient and degree of atherosclerosis, as previously described: group A = male, mild atherosclerosis, corresponding to groups I–III in the American Heart Association (AHA) classification; group B = male, advanced atherosclerosis, corresponding to groups IV–VI in the AHA classification; group C = female, mild atherosclerosis; and group D = female, advanced atherosclerosis) [10,11]. The distribution of the cases among these groups was as follows: A, 8 cases (mean 44.3 ± 10.6 years); B, 8 cases (mean 71.3 ± 3.7 years); C, 8 cases (mean 52.0 ± 3.9 years); and D, 8 cases (mean 75.0 ± 2.1 years), respectively. For RT/real-time PCR analysis, these specimens were treated according to our previous report [10]. The mRNA levels for *PTOV1* and *AR* in each sample are given as a ratio relative to *GAPDH*, and evaluated as a ratio (%) compared with that of each control cDNA.

Immunohistochemical analysis for PTOV1 protein expression in human aorta

Details of immunohistochemical procedures have been previously described [10,11]. We used immunostaining with diaminobenzidine (DAB) for immunohistochemical analysis of PTOV1 protein (using a monoclonal anti-human PTOV1 antibody; Novocastra Laboratories, Newcastle, UK) and AR (using a monoclonal antibody for human AR; Dako Corporation, Carpinteria, CA, USA). We also used double immunostaining with DAB and Vector Blue as colorimetric reagents, with a combination of monoclonal antibodies for α-smooth muscle actin (α-SMA; Dako Corporation), for macrophages (PG-M1, Dako Corporation), and for leukocytes (human leukocyte common antigen antibody (LCA; Dako Corporation) in adjacent tissue sections. After determining the areas for evaluation by simultaneous observation using a multi-headed light microscope, three authors (YN, TS, and HS) independently evaluated immunoreactivity. Scoring of immunoreactivity was performed based on our previous reports with some modifications [10,16]. When PTOV1 protein was immunolocalized to the cytoplasm, the relative immunoreactivity in each specimen was classified into the following three groups: 2 = more than 50% positive cells; 1 = more than 10% and less than 50% positive cells; and 0 = negative or less than 10% positive cells, respectively [16]. When PTOV1 protein immunoreactivity was detected in the nuclei, the relative immunoreactivity in each specimen was evaluated by the percentage of immunoreactivity, ie the labelling index (LI) [10]. When inter-observer differences were >5%, the three aforementioned authors re-evaluated these discrepant immunostained slides simultaneously using a multi-headed light microscope, and the mean value was obtained.

Statistical analysis

Values for all results were given as the mean ± standard error of the mean (SEM). Results of quantitative RT-PCR, cell count assay, and the relative immunoreactivity for protein in the nuclei were analysed using one-way analysis of variance followed by unpaired *t*-test for comparisons between two groups. Results of immunohistochemistry of cytoplasmic protein were analysed using the χ^2-test. Statistical differences between immunoreactivity for PTOV1 protein and AR were evaluated using Spearman's rank correlation. A p value <0.05 was considered significant in this study.

Results

Characterization of two VSMC cell lines

By RT-PCR analysis, both HUVS-112D cells and T/G HA-VSMC cells expressed *AR* mRNA (Figure 1A). In addition, AR protein was demonstrated in both of these cell lines by immunoblotting analysis (110 kD) (Figure 1B). Relative levels of AR mRNA and protein expression in these cells were approximately 5–10% of those in LNCaP cells that were examined in parallel (data not shown).

Gene chip microarray assay

Table 3 summarizes 11 genes that were up-regulated by testosterone treatment in both types of VSMC in duplicated microarray analysis. Among these genes, human prostate tumour overexpressed protein 1, ie *PTOV1* was detected in both of these VSMCs. Recently, *PTOV1* has been reported to be induced by androgen and to be involved in cell cycle regulation [14,15,17]. *AGTR2* was also reported to be associated with androgenic effects, but it is unknown whether *AGTR2* is involved in cell growth [18]. Therefore we focused our subsequent studies on *PTOV1* as

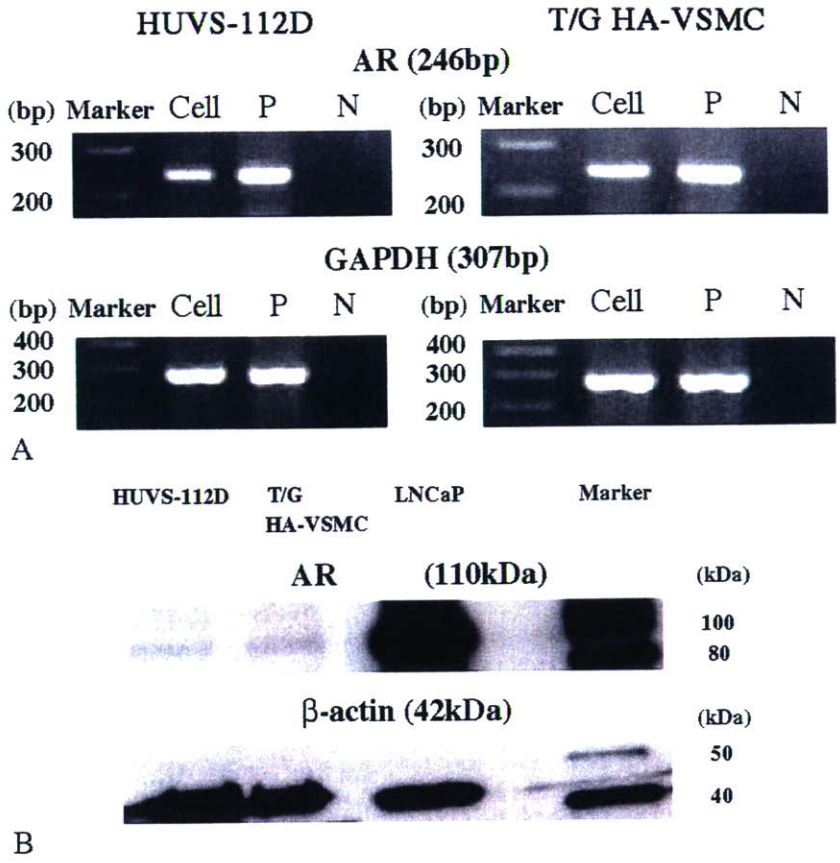

Figure 1. (A) Results of RT/real-time PCR analysis for *AR* and *GAPDH* in two cultured human VSMCs (HUVS-112D, and T/G HA-VSMC), positive controls, and negative controls. Cell = each type of cultured vascular smooth muscle cell; P = positive control (LNCaP prostate cancer cell line); N = negative control (no cDNA), respectively). (B) Immunoblotting analysis of AR and β-actin in HUVS-112D, T/G HA-VSMC, and LNCaP cells. Total protein was extracted, and 60 μg protein from each cell was loaded. Immunoblotting analysis demonstrated both AR (110 kD) and β-actin protein (42 kD) in all cells

Table 3. Ratios of gene expression determined by GeneChip microarray analysis after testosterone treatment of cultured VSMCs for 2 h

Gene symbol	HUVS-112D	T/G HA-VSMC	Function	Association with androgen (reference)
PAK7	3.9	3.6	Neurite development	Unknown
PIK3R4	1.7	3.3	Cell signalling	Unknown
CELSR1	1.9	3.1	Cell adhesion	Unknown
CACNA1G	2.5	2.9	Calcium channel	Unknown
AGTR2	2.2	2.5	Regulator of aldosterone secretion	Koike *et al* [18]
INVS	2.7	3.6	Renal tubular development	Unknown
GPR77	3.5	2.6	Cell signalling	Unknown
CASP10	3.3	2.8	Apoptosis	Unknown
AP4S1	2.1	2.5	Formation of cell structure	Unknown
T1A-2	1.7	2.7	Membrane glycoprotein	Unknown
PTOV1	1.8	2.0	Cell growth/mitogenesis	Benedit *et al* [14]

'Ratios' represent the mean ratios of expression levels of each gene mRNA in duplicate experiments compared with control.

an androgen-responsive gene possibly involved in the proliferation of human VSMCs.

PTOV1 mRNA expression in VSMCs after androgen treatment

Testosterone significantly increased *PTOV1* mRNA levels in AR-positive VSMCs compared with controls in both of these cell lines ($p < 0.05$) (Figure 2). However, testosterone with flutamide, an AR-blocker (100 nM), did not increase its mRNA expression in either of these cells ($p < 0.05$) (Figure 2).

PTOV1 siRNA transfection and cell proliferation assay

Quantitative RT-PCR analysis demonstrated that *PTOV1* mRNA levels were decreased in a dose-dependent manner in the cells transfected with *PTOV1* siRNAs (Figure 3A). After transfection of negative

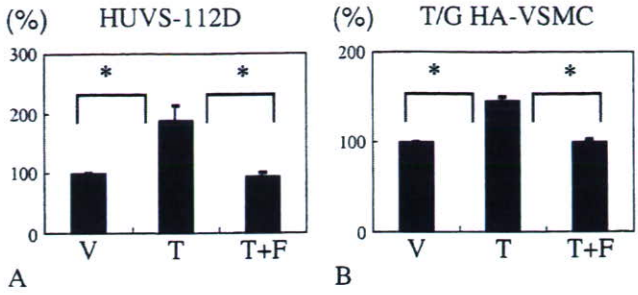

Figure 2. Results of RT/real-time PCR analysis for *PTOV1* in HUVS-112D (A) and T/G HA-VSMC cells (B) among cells treated with vehicle (V) (control), testosterone (T) alone (10 nM), and T (10 nM) with flutamide (F), an AR-blocker (100 nM), respectively after 2 h (*$p < 0.05$)

control siRNA (10 nM), testosterone promoted cell proliferation significantly in both of these cell lines ($p < 0.05$) (Figure 3B). However, testosterone with transfection of *PTOV1* siRNA (10 nM and 100 nM) did not increase cell proliferation in these two cell lines (Figure 3B).

PTOV1 mRNA expression in human aorta

The results of RT/real-time PCR analysis demonstrated the presence of specific single bands for *AR* and *PTOV1* in human aorta (Figure 4A). The relative abundance of *PTOV1* mRNA was significantly greater in male aorta with a mild degree of atherosclerotic changes (group A) than in those of other groups (groups B, C, and D)($p < 0.05$) (Figure 4B). The relative abundance of *AR* mRNA was also significantly greater in male aorta with a mild degree of atherosclerotic change (group A) than in male aorta with a severe

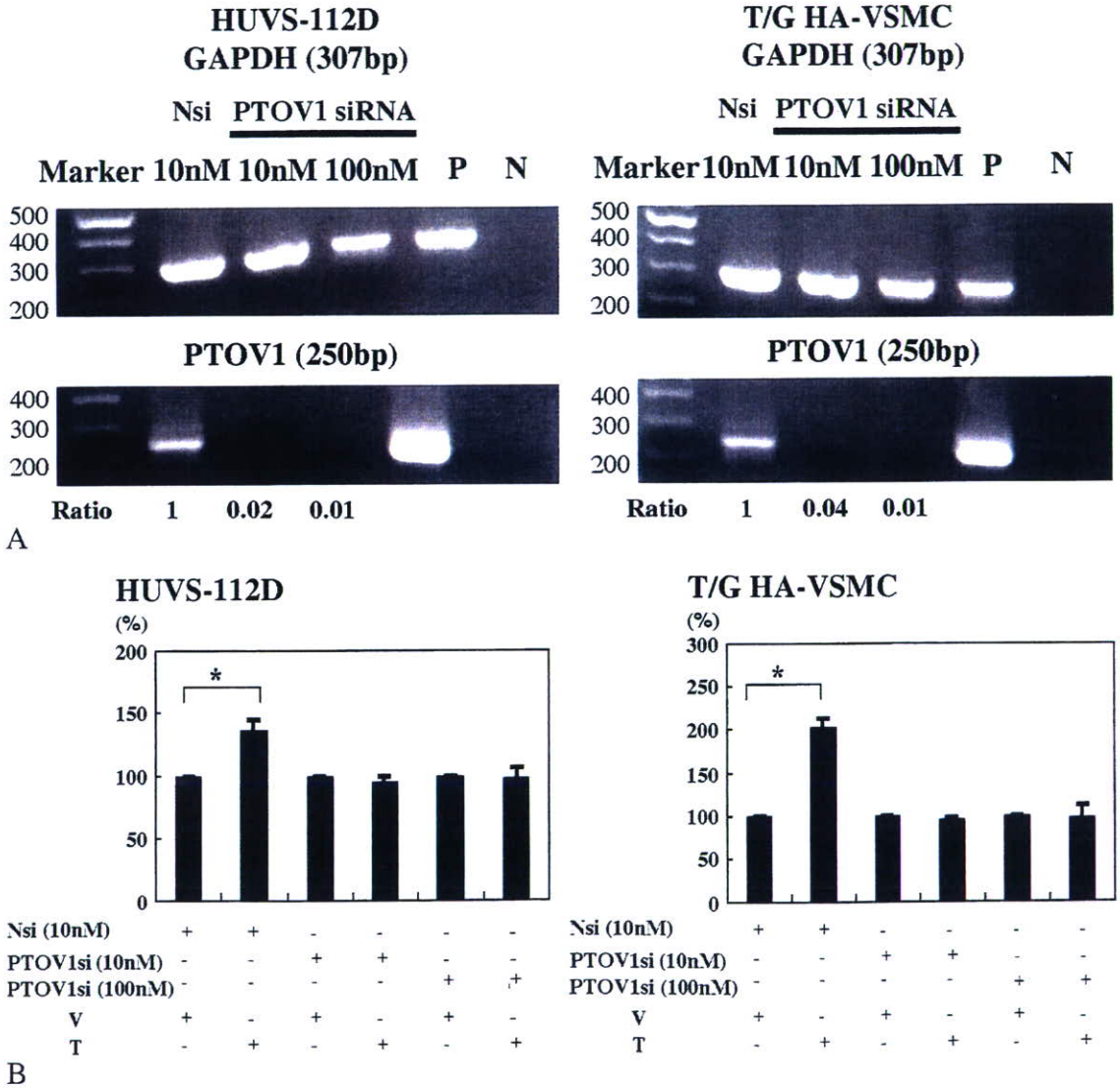

Figure 3. (A) Expression of *PTOV1* and *GAPDH* mRNAs at 24 h after transfection of *PTOV1* siRNA (10 nM or 100 nM) or negative control siRNA (Nsi) (10 nM) in HUVS-112D and T/G HA-VSMC cells detected by real-time PCR, respectively. *GAPDH* mRNA expression was monitored as an internal control. The ratio of *PTOV1/GAPDH* was calculated and values were normalized to the ratio obtained from the negative control transfection of Nsi (10 nM). P = positive controls (LNCaP prostate cancer cell lines); N = negative controls (no cDNAs), respectively. (B) The relative levels of cell numbers in HUVS-112D and T/G HA-VSMC cells among cells treated with vehicle (V) (0.1% ethanol) and testosterone (T) alone (10 nM) after transfection of *PTOV1* siRNA (PTOV1si) (10 nM or 100 nM) or negative control siRNA (Nsi) (10 nM) (*$p < 0.05$)

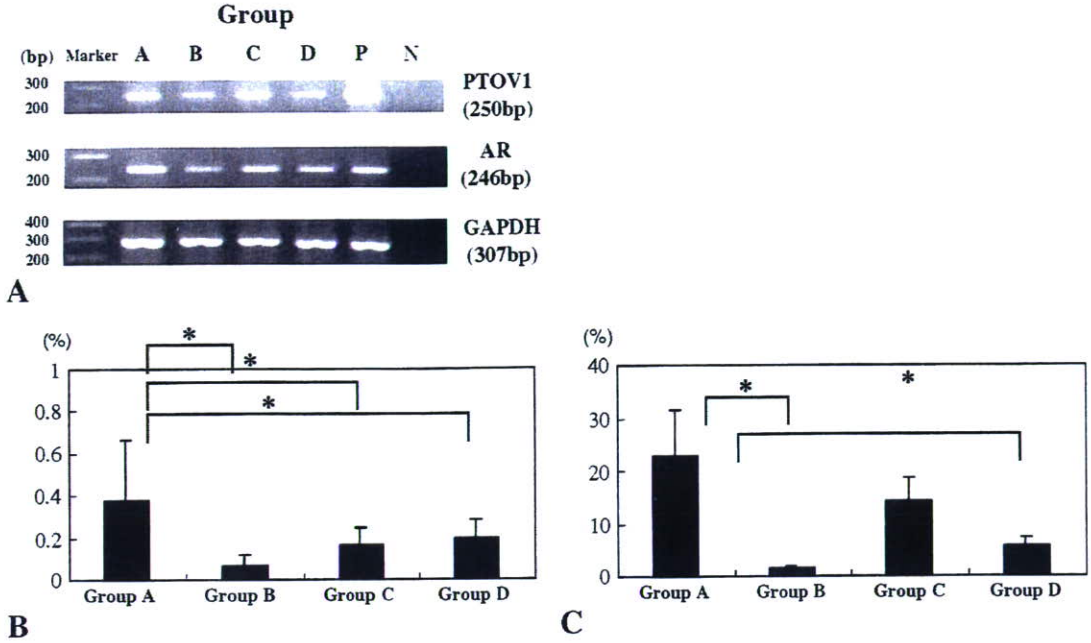

Figure 4. (A) Results of RT/real-time PCR analysis for *PTOV1* in human aortas. Bands for PCR products were detected as specific single bands (246 bp for *AR*, 250 bp for *PTOV1*, and 307bp for *GAPDH*). The amplified products were run on a 2% agarose gel stained with ethidium bromide. Representative photographs for these RT/real-time PCR gene products are illustrated. A = aorta from a 38-year-old man with mild atherosclerotic change; B = aorta from a 72-year-old man with severe atherosclerotic change; C = aorta from a 45-year-old woman with mild atherosclerotic change; D = aorta from a 76-year-old post-menopausal woman with severe atherosclerotic change; P = positive controls; N = negative controls. (B) Results for *PTOV1* mRNA expression levels ($^*p < 0.05$). (C) Results for *AR* mRNA expression levels ($^*p < 0.05$)

degree of atherosclerosis (group B) and in female aorta with a severe degree of atherosclerosis (group D) ($p < 0.05$) (Figure 4C).

Immunohistochemistry for PTOV1 in human aorta

PTOV1 protein was expressed in both the nucleus and the cytoplasm of VSMCs in each group examined (Figures 5 and 6). AR protein was expressed in the nuclei of VSMCs in each group (Figures 5 and 6). However, none of the LCA- or PG-M1-positive cells demonstrated any PTOV1 immunoreactivity (Figure 5). The relative levels of PTOV1 immunoreactivity in the nuclei of neointimal VSMCs were significantly higher in male aorta with a mild degree of atherosclerotic change (group A) than in those of the other groups examined (groups B, C, and D) (Figure 6A). In addition, AR-positive cells in the neointima were also significantly more abundant in male aorta with a mild degree of atherosclerotic changes (group A) than in those of the other groups (groups B, C, and D) ($p < 0.05$) (Figure 6E). There was also a significant positive correlation between AR and PTOV1 immunoreactivity in the nuclei of VSMCs in the neointima ($p < 0.05$) (data not shown). AR-positive cells in the tunica media were significantly more abundant in male aorta with a mild degree of atherosclerotic change (group A) than in male aorta with a severe degree of atherosclerosis (group B) and in female aorta with a mild degree of atherosclerosis (group C) ($p < 0.05$) (Figure 6F). However, there were no significant differences in PTOV1 immunoreactivity in the cytoplasm of cells in the neointima or in the nucleus and/or cytoplasm of cells in the tunica media among these groups (Figure 6B, C, and D).

Discussion

In our present study, results of both microarray and quantitative RT-PCR analyses all indicated that *PTOV1* is one of the genes induced by testosterone via AR-dependent pathways in cultured human VSMCs. In addition, siRNA analysis demonstrated that *PTOV1* is involved in AR-mediated VSMC proliferation. Results of both quantitative RT-PCR and immunohistochemical studies in human aorta obtained at autopsy further demonstrated that PTOV1, as well as AR, detected in the nuclei of neointimal VSMCs was abundant in relatively young male aorta at an early stage of atherosclerosis.

PTOV1 has been known to be involved in stimulation of cell proliferation [14,15,17]. This gene is a mitogenic factor that shuttles between nucleus and cytoplasm in a cell cycle-dependent manner in prostate carcinoma cells [14,15,17]. In addition, *PTOV1* overexpression induced cell proliferation and facilitated entry of prostate carcinoma cells into the S phase [14,15,17]. Therefore, these findings all indicated that *PTOV1* may play a very important role in the proliferation of VSMCs. However, it is also true that other atherogenic effects on human VSMCs, such as promotion of PDGF-induced VSMC proliferation,

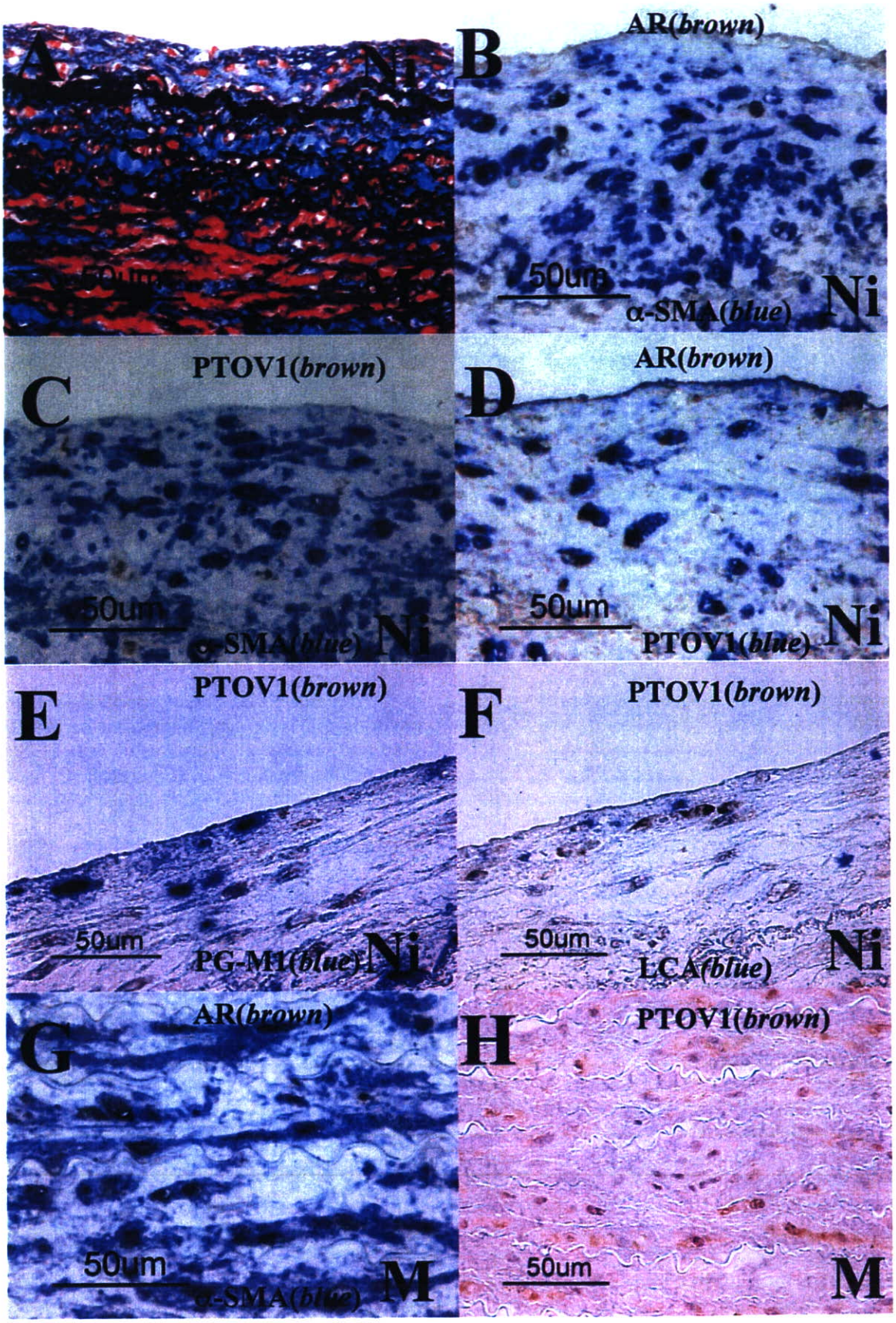

Figure 5. Modified Masson Goldner's stains (A), double-immunohistochemical staining for AR and α-muscle actin (α-SMA) (B), for PTOV1 and α-SMA (C), for AR and PTOV1 (D), for PTOV1 and PG-M1 (E), for PTOV1 and leukocyte common antigen (LCA) (F) in the neointima, double-immunohistochemical staining for AR and α-SMA (G) and immunohistochemical staining for PTOV1 (H) in the media of an abdominal aorta specimen obtained from a 38-year-old man with a mild degree of atherosclerosis (group A). Immunopositive cells appear brown as a result of DAB colorimetric reaction and blue as a result of Vector Blue colorimetric reaction. Double-immunopositive cells are confirmed. Ni = neointima; M = media